Development and Analysis of a High Fidelity Linearized J_2 Model for Satellite Formation Flying

By

SAMUEL A. SCHWEIGHART

B.S. Aeronautical and Astronautical Engineering
University of Illinois at Urbana-Champaign, 1999

SUBMITTED TO THE DEPARTMENT OF
AERONAUTICAL AND ASTRONAUTICAL ENGINEERING
IN PARTIAL FULLFILLMENT OF THE DEGREE OF

MASTER OF SCIENCE

at the

MASSACHUSETTS INSTITUTE OF TECHNOLOGY

June 2001

© 2001 Massachusetts Institute of Technology
All rights reserved

Signature of Author……
Department of Aeronautics and Astronautics
May 21st, 2001

Certified by……
Raymond J. Sedwick
Research Scientist in the Department of Aeronautics and Astronautics
Thesis Supervisor

Certified by……
David W. Miller
Associate Professor of Aeronautics and Astronautics
Director of the MIT Space Systems Laboratory

Accepted by……...
Wallace E. Vander Velde
Professor of Aeronautics and Astronautics
Chair, Committee on Graduate Students

ABSTRACT

Development and Analysis of a High Fidelity Linearized J_2 Model for Satellite Formation Flying

By

SAMUEL A. SCHWEIGHART

Submitted to the Department of Aeronautics and Astronautics
on June 8th, 2001 in Partial Fulfillment of the
Requirements for the Degree of Master of Science
at the Massachusetts Institute of Technology

With the recent flurry of research on satellite formation flying, a need has become apparent for a set of linearized equations of relative motion that capture the effect of the J_2 geopotential disturbance force. Typically, Hill's linearized equations of relative motion have been used for this analysis, but they fail to capture the effect of the J_2 disturbance force on a satellite cluster. In this thesis, a new set of constant coefficient, linearized differential equations of motion is derived. These equations are similar in form to Hill's equations, but they capture the effects of the J_2 disturbance force. The validity of these equations will be verified by comparing the mean variation in the orbital elements to the solutions of these equations. A numerical simulator will also be employed to check the fidelity of the equations. It will be shown that with the appropriate initial conditions, the new linearized equations of motion have periodic errors on the order of centimeters that do not grow in time. The new linearized equations of motion also allow for insight into the effects of the J_2 disturbance on a satellite cluster. This includes 'tumbling', the period of the relative orbit, and satellite separation due to differential J_2 effects. Overall, a new high fidelity set of linearized equations are produced that are well suited to model satellite relative motion in the presence of the J_2 disturbance force.

ACKNOWLEDGMENTS

I'd like to take the time to publicly acknowledge and thank…

My Lord, for all the gifts he has given me.

My parents, for their support and love.

Ray, my advisor, for all of his time and help on this project.

The National Science Foundation for funding this research.

The Pit Crew for making the past two years here at MIT a great place to work.

All my friends, both here at MIT and back home.

Thank you.

TABLE OF CONTENTS

TABLE OF FIGURES

Chapter 1

INTRODUCTION

Satellite formation flying is the placing of multiple satellites into nearby orbits to form 'clusters' of satellites. These clusters of satellites usually work together to accomplish a mission. There are many benefits to using multiple spacecraft as opposed to one large spacecraft. These include, but are not limited to: increased productivity, reduced mission and launch costs, graceful degradation, on-orbit reconfiguration options, and the ability to accomplish missions that would be unattainable any other way.

One example of a mission that will use formation flying is the Air Force's TechSat 21 mission [1]. The TechSat 21 mission is a distributed satellite system that is a flight demonstration of space-based radar. Interferometry will be used to detect ground-moving targets. The approach of interferometry to obtain high-resolution images is not new. It has been used in many ground-based applications, most notably in the Very Large Array [2]. The VLA is a radio observatory in New Mexico that uses 27 radio dishes, each 82 feet across, to produce an image with the same resolution as a dish 36 km wide. TechSat 21 will employ this same technique of interferometry by using up to 16 satellites in a cluster approximately 500 meters wide. These satellites will work together to produce high-resolution ground target information.

With the desire to place spacecraft into clusters, comes the need to accurately determine and control the position of satellites within the formation. In order to accomplish this, researchers initially turned to Hill's equations, also known as the Clohessy-Willshire equations. Hill's equations are a set of linearized equations that describe the relative motion of two spacecraft in similar near-circular orbits assuming Keplerian central force motion [3]. In the past Hill's equations have been used for rendezvous maneuvers, but these equations have started to find a new use in satellite formation flying.

As will be shown in Chapter 2, much research on satellite formation flying has been accomplished through the use of Hill's equations. These equations are utilized because they are easy to use. They are a set of linearized, constant coefficient differential equations. Because of this, they can be solved analytically and provide a solution that is fairly simple in form and is easy to understand. These solutions allow for an intuitive sense of the relative motion of satellites in clusters. Hill's equations are also used in the design of control laws since the most effective control schemes require a set of constant coefficient, linearized equations. These reasons and more make them the logical first choice in describing relative satellite motion.

However, while Hill's equations have proved very useful, they have several significant limitations. Since they are linear, some error is introduced into the solution. However, linearization errors are not the limiting factor. Hill's equations are derived under the assumption that the disturbance forces acting on the satellites are negligible. This assumption is usually acceptable for most relative motion problems, including rendezvous maneuvers. In rendezvous maneuvers, the spacecraft are usually spaced relatively close, and thus the differential effect on each spacecraft is small. Rendezvous maneuvers are also relatively short in duration, so errors have little time to develop.

For formation flying, the conditions are a little different. Satellites are spaced from meters to kilometers apart. Missions are also on a larger time scale, and errors begin to add up. Because of these two issues, disturbances do have a significant effect on the satellite motion.

The disturbance force cited time and time again as the preventing force from making Hill's equations a completely useful tool is the J_2 geopotential disturbance force. Because the Earth is an oblate spheroid, (it's like a squished basketball bulging out at the equator), the gravitational potential is not constant as the satellite orbits the earth. This disturbance causes many variations over time in the satellite orbital elements. Independent of satellite size or shape, the J_2 force is always a dominating presence and cannot be changed.

In the derivation of Hill's equations, the Earth is considered spherical, and the J_2 disturbance in not incorporated. Thus, they do not capture the J_2 disturbance effects. Many papers have since been written that quantify the error resulting from their use. Other papers do not use them at all, citing the fact that they do not capture the motion of the satellites correctly.

It appears that there is a need for a set of linearized equations that are as easy and useful as Hill's equations, but at the same time capture the effect of the J_2 disturbance force. In this thesis, a set of linearized, constant coefficient differential equations will be developed that capture the J_2 disturbance force.

These new equations are similar to Hill's equations in form. The radial and in-track motion is still coupled, but are separate from the cross-track direction. They are easily solvable, and the solutions look very similar to Hill's equations. However, they capture the J_2 disturbance that Hill's equations fail to capture.

Satellite formation designers will now be able to quickly and accurately predict cluster size and shape. They will also be able to design optimal control laws that take into account the effects of the effects of the J_2 disturbance force.

Finally, the new linearized equations of motion allow for some new insight into the motion of satellites under the presence of the J_2 disturbance force. Cluster 'tumbling' is discussed as a J_2 effect. The cross-track motion has also been analyzed and determined to be much more complex than previously thought.

The derivation of these equations will be presented in Chapter 3. Following in Chapter 4 is an analysis of the new linearized equations. The solutions to the new linearized equations will be compared against the mean variation in the orbital elements. Then the solutions will be compared to numerical simulation. Concluding in Chapter 5 will be a discussion of the insights gained by using the new linearized equations.

Chapter 2

PREVIOUS WORK

In this section, a brief overview will be given on a selection of papers that deal with the relative positioning, motion, and control of satellites in clusters. Some of the papers presented employ Hill's equations as their sole means of determining the satellite motion. Others cite the errors in Hill's equations, primarily due to differential J_2 forces and calculate the errors incurred by using them. Finally some use non-linear techniques to derive their solutions.

2.1 Using Hill's Equations as the Equations of Motion

There are many different ways of describing satellite motion within a cluster. In the past, when relative motion between satellites has been needed, Hill's equations have been used. This typically was for rendezvous missions where the distance separating the spacecraft was small, and the mission time relatively short. However, due to their ease of use and relatively good accuracy, they make a natural transition to satellite formation flying. Once again the relative motion between two satellites is calculated, but now they are separated by a greater distance and for longer periods of time. The following papers in this section use Hill's equations as the primary means of describing satellite motion.

2.1.1 "Relative Orbit Design Tool"

The first paper discussed is written by Tollefson [4]. He has recently created a software package for satellite formation flying. Using a graphical interface, this software package allows users to rapidly design and test satellite clusters.

In his paper, Tollefson first uses Hill's equations to describe the different types of relative orbits that are possible in a cluster. These relative orbits can be designed in the software

package, and the software is able to output the traditional orbital elements for each satellite in the cluster.

The tool also has many graphical interfaces and displays that allow the user to see the cluster in many different views. This allows a user to change the parameters of the cluster while noting the effect it has on the cluster. Finally, the tool has three additional features: a two-body orbit propagator (for elliptical reference orbits), collision detection, and the ability to output the orbital elements of the cluster into Satellite Tool Kit. Overall, the paper describes a tool that allows for the quick and easy design of satellite clusters.

2.1.2 "TechSat 21 Cluster Design Using AI Approaches and the Cornwell Metric"

The next paper is by Kong, Tollefson, Skinner, and Rosenstock [5]. In their paper, they describe an approach for choosing an optimal cluster design. Their research is primarily focused on the TechSat 21 mission.

Because of the many different configurations possible for a satellite cluster, intelligent search algorithms are utilized to choose an optimal design. Two different metrics are disused for possible use in the optimization routine: Point Spread Functions, and the Cornwell Metric. Using Hill's equations as the satellites' equations of motion, the paper shows that intelligent search algorithms are nearly as effective as evaluating the whole trade space. However, intelligent algorithms are faster by three orders of magnitude. The paper also demonstrates that there are potentially new cluster designs for the TechSat 21 mission that may be better than current designs.

2.1.3 "Geometry and Control of Satellite Formations"

A paper by Yeh and Sparks [6] utilizes Hill's equations to present some interesting geometrical relationships for satellites in clusters. For example, Hill's equations predict that 'orbits' of one satellite around another satellite are restricted to the intersection of a plane and an elliptical cylinder with an eccentricity of $\sqrt{3}/2$. This allows for some

interesting insight into which 'orbits' are possible, and which ones cannot be designed. This same technique is used to help describe satellite 'tumbling' in section 5.3.

The paper also presents a control law using Hill's equations. Disturbances and control forces are placed onto the right hand side of Hill's equations as forcing functions. These control laws allow for the cluster initialization and adjustment. The author states, that Hill's equations are a starting point for designing control laws, but also states that these control laws may be inefficient when disturbances such as the J_2 disturbance force are incorporated.

2.1.4 "Satellite Formation Flying Design and Evolution"

The paper by Sabol, Burns, and McLaughlin, [7] gives a brief overview on the evolution of cluster design, and utilizes Hill's equations to describe the different types of cluster designs. Each cluster design is placed into a simulator with realistic dynamics, and the results from each simulation are presented and discussed. The effects of the J_2 disturbance force are noted and a control scheme is presented for formation keeping.

Using Gauss' variation of parameters, the minimum Δv needed to counteract the J_2 disturbance force was calculated. This required Δv provides a minimum Δv needed for station keeping in the presence of the J_2 disturbance force.

2.1.5 "Linear Control of Satellite Formation Flying"

In this paper by Sparks [8], Hill's equations are once again used to define the motion of satellites in the cluster. The J_2 disturbance force was labeled as the most destabilizing perturbation. Just like in the previous paper, Gauss' variation of parameters was used to derive a minimum value for the total Δv needed to counteract the effects of the J_2 disturbance.

A discrete time linear control law was then developed. This control law was placed into a simulator and was able to produce approximately the same Δv as the theoretical minimum given by Gauss' variation of parameters.

2.2 Quantifying the Errors of Utilizing Hill's Equations

While the previous papers have used Hill's equations as a means of describing satellite motion, other papers analyze the errors that are incurred by using them.

2.2.1 "Gravitational Perturbations, Nonlinearity and Circular Orbit Assumption Effects on Formation Flying Control Strategies"

The J_2 disturbance force affects each satellite in a cluster differently. These differential forces cause the cluster to change shape and separate. An analytical method by Alfriend, Schaub, and Gim [9] is used to evaluate the differential forces, and the effects of using Hill's equations.

In the paper, a state transition matrix is calculated that relates the changes in the orbital elements to changes in the local coordinate frame. The resulting equations are compared to Hill's equations in the presence of J_2 perturbations, and eccentric reference orbits. The results showed that using this state transition matrix provided better results than that obtained with Hill's equations.

2.3 Eccentric Orbits

Due to the assumptions made in the derivation of Hill's equations, satellite clusters have traditionally been considered to be in near-circular obits. However, there are some benefits to placing satellite clusters into eccentric orbits. This allows for longer dwell time over regions of interest, and shorter occultation time. Since Hill's equations are based on a circular reference orbit, they fail for eccentric reference orbits.

First introduced by Lauden [10], time varying linear equations of motion can be developed utilizing an elliptical reference orbit. The resulting differential equations, while no longer time-invariant can be solved analytically.

2.3.1 "Relative Dynamics & Control of Spacecraft Formations in eccentric Orbits"

Inalhan and Hall [11] have expanded the topic of eccentric reference orbits to incorporate satellite clusters. In their paper, they derive the linearized time varying equations of motion, and present the homogenous solutions. They also present initial conditions that produce periodic solutions, thus preventing satellites from drifting apart due to different orbital periods. The solutions to the elliptical linearized equations are then compared to Hill's equations for modeling satellite clusters in elliptical orbits. The errors incurred by utilizing Hill's equations are presented.

2.4 Non-Linear Techniques

2.4.1 "J_2 Invariant Relative Orbits for Spacecraft Formations"

The J_2 disturbance causes many changes to a satellite's orbital elements over time. This includes precession of the ascending node, argument of periapsis, and changes to the mean motion. In a satellite cluster, the differential changes in the orbital elements causes satellites clusters to change form and drift apart.

In this paper by Schaub and Alfriend [12], an analytical technique is used to derive a class of orbits that are termed 'J_2 invariant' orbits. Satellites placed into 'J_2 invariant' orbits are not immune to the J_2 disturbance force, but instead two satellites placed into these orbits will have the same drift, and thus the cluster remains together. The 'J_2 invariant' orbits are created by using two first order conditions that determine the correct differences in semi-major axis, eccentricity, and inclination.

2.4.2 "Impulsive Spacecraft Formation Flying Control to Establish Specific Mean Orbital Elements"

In this paper by Schaub and Alfriend [13], an impulsive control algorithm is developed using mean orbital elements. The change from osculating orbital elements to mean orbital elements seems to have a two-fold purpose. The first is that small periodic

variations are not captured by the control system and thus propellant is not wasted counteracting these variations. Instead only the secular drift in any of the orbital elements is corrected for.

The second reason for switching to mean orbital elements is because impulsive maneuvers are only applied once or twice during an orbital period. If the amount of thrust applied is dependent on the current orbital elements, the average orbital elements need to be used otherwise periodic variations may cause errors.

The reason why impulsive maneuvers are only performed once or twice an orbit, is because the paper once again uses Gauss' variation of parameters. This allows the controller to choose almost independently which orbital element to change and when to apply that thrust at the most opportune time. The opportune time to thrust usually only happens once or twice an orbit.

Numerical simulations were conducted to verify that the controller was capable of controlling the variation in the mean orbital elements in the presence of disturbances, and cluster misalignments.

2.5 Linearized Equations of Motion that Incorporate the J_2 Disturbance Force

2.5.1 "Mitigation of Differential Perturbations in Clusters of Formation Flying Satellites"

This paper by Sedwick, Miller and Kong [14] analyzed an assortment of perturbation effects of a satellite cluster. These included a non-spherical Earth, atmospheric drag, solar radiation pressure, and magnetic field interactions. This was first done by using a non-dimensional approach to determine the scaling of each perturbation effect.

The next section of the paper looks at each perturbation effect in more detail. Focusing on the TechSat 21 mission, only polar orbits were analyzed, and only in-plane disturbances were accounted for. For the J_2 disturbance analysis, the J_2 disturbance force

is added to the right side of Hill's equations as a disturbance force. In order to calculate the differential J_2 effects, a nominal trajectory is projected into the J_2 force to produce a new forcing function. The resonant terms in this forcing function are responsible for the secular drift in the relative motion, and the Δv needed to counteract these forces is presented.

The other disturbance forces, including the error due to the linearization, are also looked at in more detail. The resulting total Δv necessary for station keeping is analyzed and presented for the TechSat 21 mission.

2.5.2 "A Perturbative Analysis of Geopotential Disturbances for Satellite Formation Flying"

Written by this author, the paper **[15]** is written on the same subject as this thesis. In this paper, both the gradient of the J_2 force and the gradient of the spherical gravitational potential are incorporated to from a new set of linearized equations. This is the same derivation that is presented in the next chapter. At the time of the writing, the cross-track motion was just being understood, and was not fully explained. This thesis will complete the analysis of the cross-track motion and provides the final linearized equations of motion.

2.6 Conclusion

There has been a recent flurry of research on satellite formation flying. This research falls into three general categories: papers that utilize Hill's equations, papers that show Hill's equations do not capture the J_2 disturbance effects, and papers that use a non-linear method of capturing the J_2 disturbance effects.

From this survey of current research, there appears to be a need for a set of linearized equations that are easy to use, but at the same time are able to capture the J_2 disturbance. In the next chapter a set of linearized equations of motion will be presented that captures the J_2 disturbance force but at the same time is as easy to use as Hill's equations.

Chapter 3

DERIVATION OF THE NEW LINEARIZED EQUATIONS OF MOTION

In this chapter, a new set of linearized equations of motion will be developed. These equations will be like Hill's equations in form, but will also capture the effects of the J_2 disturbance force.

3.1 Approach Overview

The first step in the derivation is to write the equation of motion of a satellite under the influence of the J_2 disturbance in its simplest form, where $\vec{g}(\vec{r})$ is the gravitational force due to a spherical Earth, and $\vec{J}_2(\vec{r})$ is the J_2 disturbance force.

$$\ddot{\vec{r}} = \vec{g}(\vec{r}) + \vec{J}_2(\vec{r}) \tag{3.1}$$

While this equation completely describes the motion of a satellite under the influence of the J_2 disturbance, it is not necessarily useful. First it cannot be solved analytically. Second, it is not useful in visualizing the relative motion that is present in satellite clusters.

The solution to these problems is to introduce a reference orbit. This reference orbit can be tailored to be any type of orbit. In this thesis, four different reference orbits will be used: an unperturbed circular orbit (Hill's Equations), a circular orbit with a modified period (Solution 1), a circular orbit with modified period, inclination, and longitude of the ascending node (Solution 2), and finally the center of the cluster itself (Relative Motion).

The next step in the derivation is to linearize both the standard gravitational term and the J_2 disturbance around this reference orbit.

$$\ddot{\vec{r}} = \vec{g}(\vec{r}_{ref}) + \nabla\vec{g}(\vec{r}_{ref})\cdot\vec{x} + \vec{J}_2(\vec{r}_{ref}) + \nabla\vec{J}_2(\vec{r}_{ref})\cdot\vec{x} \tag{3.2}$$

$$\text{where} \quad \vec{r} - \vec{r}_{ref} = \vec{x} \tag{3.3}$$

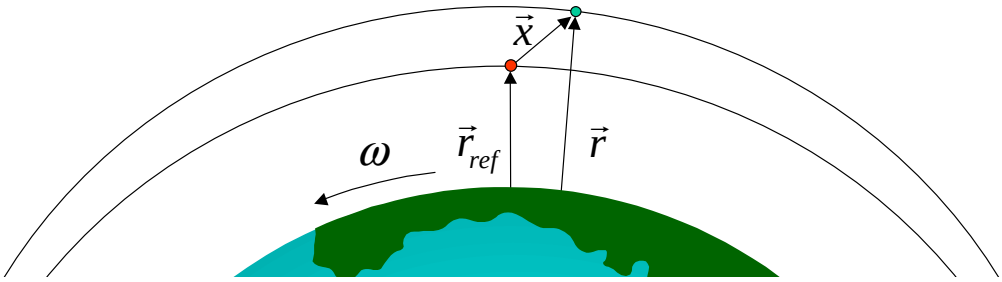

Figure 3-1 : The Reference Orbit

Since we are interested in only the relative motion between the satellite and the reference orbit, we subtract off the motion of the reference orbit from the equation of motion of the satellite.

$$\ddot{\vec{r}} - \ddot{\vec{r}}_{ref} = \vec{g}(\vec{r}_{ref}) + \nabla\vec{g}(\vec{r}_{ref})\cdot\vec{x} + \vec{J}_2(\vec{r}_{ref}) + \nabla\vec{J}_2(\vec{r}_{ref})\cdot\vec{x} - \ddot{\vec{r}}_{ref} \tag{3.4}$$

Which can be simplified to

$$\ddot{\vec{x}} = \vec{g}(\vec{r}_{ref}) + \nabla\vec{g}(\vec{r}_{ref})\cdot\vec{x} + \vec{J}_2(\vec{r}_{ref}) + \nabla\vec{J}_2(\vec{r}_{ref})\cdot\vec{x} - \ddot{\vec{r}}_{ref} \tag{3.5}$$

In the rotating coordinate system of the reference orbit, the initial equation of motion is

$$\ddot{\vec{x}} + 2\vec{\omega}\times\dot{\vec{x}} + \dot{\vec{\omega}}\times\vec{x} + \vec{\omega}\times(\vec{\omega}\times\vec{x}) = \vec{g}(\vec{r}_{ref}) + \nabla\vec{g}(\vec{r}_{ref})\cdot\vec{x} + \vec{J}_2(\vec{r}_{ref}) + \nabla\vec{J}_2(\vec{r}_{ref})\cdot\vec{x} - \ddot{\vec{r}}_{ref} \tag{3.6}$$

It will be shown later that $\nabla\vec{J}_2(\vec{r}_{ref})$ is not constant, and since we are looking for constant coefficients, the time average of the gradient is taken. The resulting equation is

$$\begin{aligned} &\ddot{\vec{x}} + 2\vec{\omega}\times\dot{\vec{x}} + \dot{\vec{\omega}}\times\vec{x} + \vec{\omega}\times(\vec{\omega}\times\vec{x}) = \\ &\vec{g}(\vec{r}_{ref}) + \nabla\vec{g}(\vec{r}_{ref})\cdot\vec{x} + \vec{J}_2(\vec{r}_{ref}) + \frac{1}{2\pi}\int_0^{2\pi}\nabla\vec{J}_2(\vec{r}_{ref})\,d\theta\cdot\vec{x} - \ddot{\vec{r}}_{ref} \end{aligned} \tag{3.7}$$

Equation (3.7) forms the basic equation that will be used throughout this paper. The main variations to it will be in the choice of the reference orbit, and corrections to the cross-track motion. These topics and a more detailed analysis are discussed in section 3.3-3.6

3.2 The Coordinate System

Before going through a detailed analysis, the four coordinate systems used throughout this thesis will be described. One system is an inertial coordinate system used to represent the absolute position of the reference orbit while the other three coordinate systems are body fixed coordinate systems.

3.2.1 The $\hat{X}$ - $\hat{Y}$ - $\hat{Z}$ Inertial Coordinate System

The $\hat{X} - \hat{Y} - \hat{Z}$ inertial coordinate system is an Earth centered system. The $\hat{X} - \hat{Y}$ plane coincides with the equatorial plane, and the $\hat{Z}$ vector points through the North Pole. See Figure 3-2.

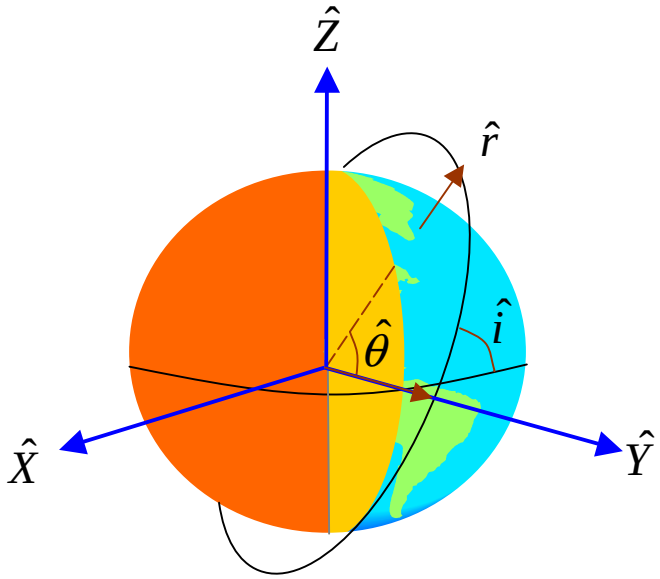

Figure 3-2 : The $\hat{X}$ - $\hat{Y}$ - $\hat{Z}$ and $\hat{r}$ - $\hat{\theta}$ - $\hat{i}$ Coordinate Systems

3.2.2 The $\hat{r}$ - $\hat{\theta}$ - $\hat{i}$ Body Fixed Coordinate System

The second coordinate system used is a spherical coordinate system. The $\hat{r}$ points in the radial direction, $\hat{i}$ is the azimuthal angle measured around the line of nodes, and $\hat{\theta}$ is the co-latitude measured from the ascending node which acts as the "pole" of the spherical system. See Figure 3-2.

3.2.3 The $\hat{R}$ - $\hat{T}$ - $\hat{N}$ Body Fixed Coordinate System

The third coordinate system is a body fixed coordinate system with the origin located at the reference satellite. The $\hat{R}$ vector (radial) points in the radial direction. The $\hat{N}$ vector (normal) is perpendicular to the orbital plane and points in the direction of the angular momentum vector. Finally the $\hat{T}$ vector (tangential) completes the orthogonal triad, and points in the direction of movement. See Figure 3-3.

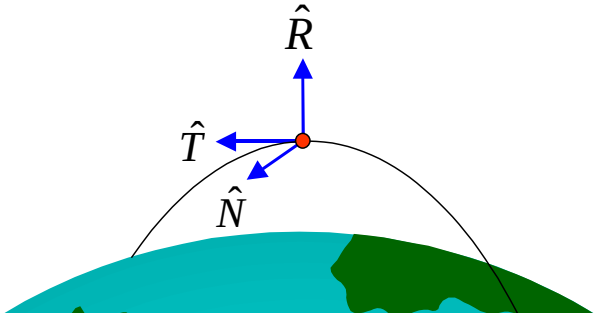

Figure 3-3 : The $\hat{R}$ - $\hat{T}$ - $\hat{N}$ Coordinate System

3.2.4 The $\hat{x}$ - $\hat{y}$ - $\hat{z}$ Body Fixed Coordinate System

The fourth and final coordinate system is also a body fixed coordinate system that is very much like the $\hat{R} - \hat{T} - \hat{N}$ coordinate system. The $\hat{x}$ vector points in the $\hat{R}$ direction, the $\hat{y}$ vector points in the $\hat{T}$ direction and the $\hat{z}$ vector points in the $\hat{N}$ direction. However, with the $\hat{x} - \hat{y} - \hat{z}$ coordinate system, the stipulation is made that it is a curvilinear coordinate system. The $\hat{x}$ vector remains unchanged, however the $\hat{y}$ and the $\hat{z}$ vector 'curve' around the orbit. In this way, the coordinate system is very much like a spherical coordinate system. See Figure 3-4.

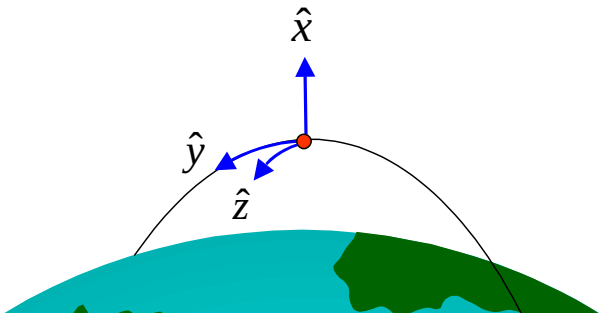

Figure 3-4 : The $\hat{x}$ - $\hat{y}$ - $\hat{z}$ Coordinate System

3.2.5 Converting Between the Body Fixed Coordinate Systems

Conversion between the body fixed coordinate systems is fairly straightforward. The radial vector in each coordinate system completely coincides. The $\hat{T}$ vector, $\hat{y}$ vector, and $\hat{\theta}$ all coincide; and the $\hat{N}$ vector, the $\hat{z}$ vector and the $\hat{i}$ vector all coincide. The only discrepancy comes from the fact that the $\hat{R}-\hat{T}-\hat{N}$ coordinate system was not defined as a curvilinear system but as rectangular.

However, the only use of the $\hat{R}-\hat{T}-\hat{N}$ is when the J_2 disturbance force is presented. This does not pose a problem because only a direction is calculated using this coordinate system and not a position. Therefore one can freely switch between the $\hat{R}-\hat{T}-\hat{N}$ system and any of the other body fixed coordinate systems described here when describing a direction or a force.

3.3 Detailed Derivation – Absolute Motion – Solution 1

Section 3.3 will present the initial derivation of the new linearized equations of motion. The steps followed here will be the same as outlined in section 3.1. Each step will be shown in more detail, and a reference orbit will be chosen. The result will be a set of linearized, constant coefficient differential equations. The analytic solution to these equations will also be presented.

3.3.1 The Basic Equations of Motion

The first step is to start off with the analytical equation of motion

$$\ddot{\vec{r}} = \vec{g}(\vec{r}) + \vec{J}_2(\vec{r}) \tag{3.8}$$

where $\vec{g}(\vec{r})$ is the gravitational force due to a spherical Earth,

$$\vec{g}(\vec{r}) = -\frac{\mu}{r^2}\hat{r} \tag{3.9}$$

and $\vec{J}_2(\vec{r})$ is the force due to the J_2 disturbance [3].

$$\begin{aligned}\vec{J}_2(\vec{r}) = -\frac{3}{2}\frac{J_2 \mu R_e^2}{r^4}[&(1-3Sin^2 i\ Sin^2\theta)\hat{R} \\ &+(2\,Sin^2 i\ Sin\theta\ Cos\theta)\hat{T} + (2\,Sin\,i\ Cos\,i\ Sin\theta)\,\hat{N}]\end{aligned} \tag{3.10}$$

where R_e is the radius of the Earth.

3.3.2 The Unperturbed Circular Reference Orbit

The next step is to introduce the reference orbit. For simplicity, a circular reference orbit only under the gravitational influence of a spherical Earth is initially used. This is the same reference orbit used in Hill's equations. The position of the reference orbit is denoted as $\vec{r}_{ref}$.

$$\ddot{\vec{r}}_{ref} = \vec{g}(\vec{r}_{ref}) \tag{3.11}$$

3.3.3 Linearization of the Gravitational Terms

The next step in the derivation is to linearize the gravitational terms with respect to the reference orbit. The resulting equation of motion is

$$\ddot{\vec{r}} = \vec{g}(\vec{r}_{ref}) + \nabla\vec{g}(\vec{r}_{ref})\cdot\vec{x} + \vec{J}_2(\vec{r}_{ref}) + \nabla\vec{J}_2(\vec{r}_{ref})\cdot\vec{x} \tag{3.12}$$

Using a spherical coordinate system ($\hat{r} - \hat{\theta} - \hat{i}$) the gradient of the $\vec{g}(\vec{r})$ gravitational force is calculated. The result is a 2nd order tensor.

$$\nabla \vec{g}(\vec{r}) = \begin{bmatrix} 2\frac{\mu}{r} & 0 & 0 \\ 0 & -\frac{\mu}{r} & 0 \\ 0 & 0 & -\frac{\mu}{r} \end{bmatrix} \tag{3.13}$$

The J_2 disturbance force (equation (3.10)) is given in $\hat{R} - \hat{T} - \hat{N}$ coordinates. However the equation can be transferred directly to a $\hat{r} - \hat{\theta} - \hat{i}$ coordinate system without any loss of generality. The resulting gradient is

$$\nabla \vec{J}_2(r,\theta,i) = \frac{6\mu J_2 R_e^2}{r_{ref}^5} \begin{bmatrix} (1-3Sin^2 i\ Sin^2\theta) & Sin^2 i\ Sin\,2\theta & Sin\,2i\ Sin\,\theta \\ Sin^2 i\ Sin\,2\theta & -\frac{1}{2} - Sin^2 i\,(\frac{1}{2} - \frac{7}{4}Sin^2\theta) & -\frac{Sin\,2i\ Cos\,\theta}{4} \\ Sin\,2i\ Sin\,\theta & -\frac{Sin\,2i\ Cos\,\theta}{4} & -\frac{3}{4} - Sin^2 i\,(\frac{1}{2} + \frac{5}{4}Sin^2\theta) \end{bmatrix} \tag{3.14}$$

3.3.4 Relative Motion

As in the derivation of Hill's equations, motion is taken with respect to the reference orbit. This relative motion is denoted as $\vec{x}$. See Figure 3-1

$$\vec{x} = \vec{r} - \vec{r}_{ref} \tag{3.15}$$

Since the reference orbit is rotating, rotational terms are needed when calculating the relative motion of the satellites. Note the '*rel*' subscripts will be dropped in the remainder of the text.

$$\ddot{\vec{x}}_{rel} = \ddot{\vec{r}} - \ddot{\vec{r}}_{ref} - 2\vec{\omega} \times \dot{\vec{x}}_{rel} - \dot{\vec{\omega}} \times \vec{x} - \vec{\omega} \times (\vec{\omega} \times \vec{x}) \tag{3.16}$$

$\vec{\omega}$ is the rotational rate of the body fixed coordinate system, and thus the angular velocity of the coordinate system. For a circular reference orbit

$$\vec{\omega} = \sqrt{\frac{\mu}{r_{ref}^3}}\,\hat{z} = n\,\hat{z} \tag{3.17}$$

Substituting equation (3.12) into equation (3.16) and re-arranging the terms yields

$$\ddot{\vec{x}} + 2\vec{\omega}\times\dot{\vec{x}} + \dot{\vec{\omega}}\times\vec{x} + \vec{\omega}\times(\vec{\omega}\times\vec{x}) = \vec{g}(\vec{r}_{ref}) + \nabla\vec{g}(\vec{r}_{ref})\cdot\vec{x} + \vec{J}_2(\vec{r}_{ref}) + \nabla\vec{J}_2(\vec{r}_{ref})\cdot\vec{x} - \ddot{\vec{r}}_{ref} \tag{3.18}$$

3.3.5 Time Averaging the J_2 Gradient Term

Equation (3.18) is a linearized equation of motion, however, the problem arises that $\nabla\vec{J}_2(\vec{r}_{ref})$ is not constant except for equatorial orbits. An approximate solution to this problem is to take the time average of the $\nabla\vec{J}_2(\vec{r})$ term.

$$\frac{1}{2\pi}\int_0^{2\pi}\nabla\vec{J}_2(\vec{r})\,d\theta = \frac{\mu}{r^3}\begin{bmatrix} 4s & 0 & 0 \\ 0 & -s & 0 \\ 0 & 0 & -3s \end{bmatrix} \tag{3.19}$$

$$\text{where } s \equiv \frac{3J_2R_e^2}{8r^2}(1+3\,Cos\,2i)$$

Equation (3.18) now becomes

$$\begin{aligned}&\ddot{\vec{x}} + 2\vec{\omega}\times\dot{\vec{x}} + \dot{\vec{\omega}}\times\vec{x} + \vec{\omega}\times(\vec{\omega}\times\vec{x}) \\ &\quad = \vec{g}(\vec{r}_{ref}) + \nabla\vec{g}(\vec{r}_{ref})\cdot\vec{x} + \vec{J}_2(\vec{r}_{ref}) + \frac{1}{2\pi}\int_0^{2\pi}\nabla\vec{J}_2(\vec{r}_{ref})\,d\theta\cdot\vec{x} - \ddot{\vec{r}}_{ref}\end{aligned} \tag{3.20}$$

3.3.6 Adjusting the Period of the Reference Orbit

Under the influence of the J_2 disturbance force, the perturbed satellite will have a different orbital period than when unperturbed. Because of this discrepancy, the satellites in the cluster drift from the reference orbit and eventually the linearized equations break

down. To fix this problem, the period of the reference orbit must be adjusted to match the period of the satellites in the cluster.

The change in period due to the J_2 disturbance can be found from the average J_2 force (not to be confused with the time average of the gradient of the J_2 term taken above). The equation of motion of the reference orbit, see equation (3.11), now becomes

$$\ddot{\vec{r}}_{ref} = \vec{g}(\vec{r}_{ref}) + \frac{1}{2\pi}\int_0^{2\pi} \vec{J}_2(\vec{r}_{ref})\, d\theta \tag{3.21}$$

where

$$\begin{aligned} &\frac{1}{2\pi}\int_0^{2\pi} \vec{J}_2(\vec{r})\; d\theta = -n^2 r\, s\, \hat{x} \\ &s = \frac{3J_2R_e^2}{8r^2}(1+3\,Cos\,2i) \end{aligned} \tag{3.22}$$

Now that the reference orbit has a new period, the angular velocity vector of the rotating coordinate system must also be updated.

$$\vec{\omega}\times(\vec{\omega}\times\vec{r}_{ref}) = \frac{\mu}{r_{ref}^2}\hat{r} + \frac{1}{2\pi}\int_0^{2\pi} \vec{J}_2(\vec{r}_{ref})\; d\theta \tag{3.23}$$

which gives

$$\begin{aligned} &\vec{\omega} = n\, c\, \hat{z} \\ &c \equiv \sqrt{1+s} \end{aligned} \tag{3.24}$$

3.3.7 Final Solution – Circular Reference Orbit – Solution 1

Equation (3.20) becomes

$$\begin{aligned} &\ddot{\vec{x}} + 2\vec{\omega}\times\dot{\vec{x}} + \dot{\vec{\omega}}\times\vec{x} + \vec{\omega}\times(\vec{\omega}\times\vec{x}) = \\ &\qquad \nabla\vec{g}(\vec{r}_{ref})\cdot\vec{x} + \vec{J}_2(\vec{r}_{ref}) + \frac{1}{2\pi}\int_0^{2\pi}\nabla\vec{J}_2(\vec{r}_{ref})\, d\theta\cdot\vec{x} - \frac{1}{2\pi}\int_0^{2\pi}\vec{J}_2(\vec{r}_{ref})\, d\theta \end{aligned} \tag{3.25}$$

Substituting in all of the terms the resulting equations of motion are (in $\hat{x}-\hat{y}-\hat{z}$ coordinates)

$$\ddot{x}-2(nc)\dot{y}-(5c^2-2)n^2x=-3n^2J_2\frac{R_e^2}{r_{ref}}\left(\frac{1}{2}-\frac{3\,Sin^2i\;Sin^2(nct)}{2}-\frac{(1+3\,Cos\,2i)}{8}\right)$$

$$\ddot{y}+2(nc)\dot{x}=-3n^2J_2\frac{R_e^2}{r_{ref}}Sin^2i\;Sin(nct)\;Cos(nct) \qquad (3.26)$$

$$\ddot{z}+(3c^2-2)\,n^2z=-3n^2J_2\frac{R_e^2}{r_{ref}}Sin\,i\;Cos\,i\;Sin(nct)$$

Because these equations are linear, constant coefficient differential equations, they can be easily solved. The results are presented below. The initial conditions, $\dot{x}_0$ & $\dot{y}_0$, that specify no drift and no offset in any direction over time have been calculated and are also presented below.

$$x=(x_0-\alpha)\,Cos(nt\sqrt{1-s})+\frac{\sqrt{1-s}}{2\sqrt{1+s}}y_0\,Sin(nt\sqrt{1-s})+\alpha\,Cos(2nt\sqrt{1+s})$$

$$y=-\frac{2\sqrt{1+s}}{\sqrt{1-s}}(x_0-\alpha)\;Sin(nt\sqrt{1-s})+y_0\,Cos(nt\sqrt{1-s})+\frac{1+3s}{2(1+s)}\alpha\,Sin(2nt\sqrt{1+s})$$

$$z=z_0\,Cos(nt\sqrt{1+3s})+\frac{\dot{z}_0}{n\sqrt{1+3s}}Sin(nt\sqrt{1+3s})+$$
$$\beta(\sqrt{1+s}\;\;Sin(nt\sqrt{1+3s})-\sqrt{1+3s}\;Sin(nt\sqrt{1+s})) \qquad (3.27)$$

$$\dot{y}_0=-2nc\,x_0+\frac{3n\,J_2R_e^2}{8c\,r_{ref}}(1-Cos\,2i) \qquad \dot{x}_0=y_0\,n\,(\frac{1-s}{2c})$$

$$\alpha=\frac{3J_2\,R_e^2}{8r_{ref}\,(3+5s)}(1-Cos\,2i_{ref}) \quad \beta=\frac{3J_2\,R_e^2\;Sin\,2i_{ref}}{4r_{ref}\,s\sqrt{1+3s}}$$

$$s=\frac{3J_2R_e^2}{8r_{ref}^2}(1+3\,Cos\,2i_{ref}) \quad c=\sqrt{1+s}$$

3.4 Detailed Derivation Cont. – Absolute Motion – Solution 2

While the above equations of motion are a vast improvement over Hill's equations when incorporating the J_2 disturbance force, more can be done. Even though the orbital period of the reference orbit has been adjusted to match the perturbed satellite they still drift apart due to separation of the longitude of the ascending node. This section will derive an expression for a new reference orbit that has the same drift in the longitude of the ascending node as the perturbed satellite. This will be accomplished by using mean variations in the orbital elements. It should be noted that this expression is only an approximate solution to the new reference orbit and modeling errors are introduced.

3.4.1 Re-adjusting the Reference Orbit

While the current reference orbit and the satellites in the cluster have the same orbital period, they still drift apart. This is due to the fact that the longitude of the ascending node of a satellite will drift under the influence of the J_2 disturbance.

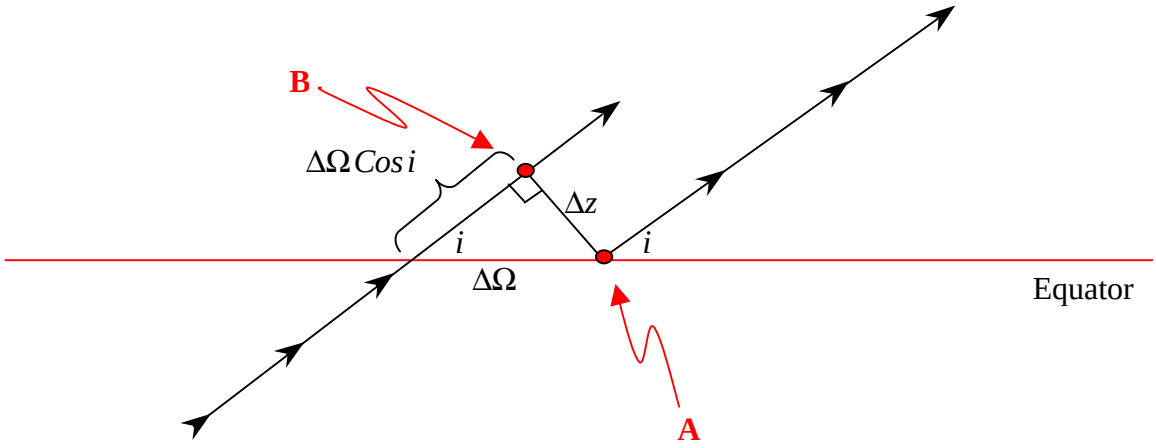

Figure 3-5 : The Effects of a Changing Argument of Periapsis

If both the reference orbit and a satellite in the cluster start at point A, after one orbital period the perturbed satellite will be at point B while the current reference orbit will return to point A. The satellites are now separated by a distance Δz. After two orbital

periods, the satellites will be separated by an additional Δz, and this process will continue causing the satellites to drift farther and farther apart. See Figure 3-5.

Because the J_2 disturbance force is causing this separation, the solution to this problem is to determine the aspect of the J_2 disturbance that causes the drift in the $\hat{z}$ direction and incorporate it into the reference orbit.

Using Gauss' mean variation in the orbital elements [3], the normal component of the J_2 force is responsible for the drift in the longitude of the ascending node. Applying the normal component of the J_2 disturbance force to the reference orbit results in

$$\ddot{\vec{r}}_{ref} = \vec{g}(\vec{r}_{ref}) + \frac{1}{2\pi}\int_0^{2\pi} \vec{J}_2(\vec{r}_{ref})\, d\theta + \vec{J}_2(\vec{r}_{ref}) \cdot \hat{N} \tag{3.28}$$

With the addition of this force onto the reference orbit, both the satellite and the reference orbit will have a drift in the longitude of the ascending node. Thus, the satellites will not drift apart. It should be noted that differential J_2 effects due to the perturbed satellite and the reference orbit having different inclinations may still cause differential drift in the two orbits, but this drift is on a much smaller scale and will be accounted for in section 3.5

3.4.2 Describing the New Reference Orbit

With the addition of the new forcing term onto the reference orbit, it is not easy to analytically describe the motion of the new reference orbit. One solution is to look at the mean variation of the orbital elements.

The position of the reference satellite in $\hat{X} - \hat{Y} - \hat{Z}$ Earth-centered inertial coordinates is [3]

$$\begin{aligned} \vec{r}_{ref} = {} & r_{ref}(Cos\,\Omega\, Cos\,\theta - Sin\,\Omega\, Sin\,\theta\, Cos\,i)\hat{X} \\ & + r_{ref}(Sin\,\Omega\, Cos\,\theta + Cos\,\Omega\, Sin\,\theta\, Cos\,i)\hat{Y} \\ & + r_{ref}(Sin\,\theta\, Sin\,i)\hat{Z} \end{aligned} \tag{3.29}$$

The normal component of the J_2 disturbance has an effect on four out of the six orbital elements:

$$\begin{aligned}
\left(\frac{\partial i}{\partial t}\right)_{\substack{Normal\\Force}} &\approx -\frac{3\sqrt{\mu}J_2R_E^2}{r^{7/2}} Sin\,i\; Cos\,i\; Sin\,\theta\; Cos\,\theta \\
\left(\frac{\partial \Omega}{\partial t}\right)_{\substack{Normal\\Force}} &\approx -\frac{3\sqrt{\mu}J_2R_E^2}{r^{7/2}} Cos\,i\; Sin^2\theta \\
\left(\frac{\partial \omega}{\partial t}\right)_{\substack{Normal\\Force}} &\approx \frac{3\sqrt{\mu}J_2R_E^2}{r^{7/2}} Cos^2 i\; Sin^2\theta \\
\left(\frac{\partial \theta}{\partial t}\right)_{\substack{Normal\\Force}} &\approx \left(\frac{\partial \omega}{\partial t}\right)_{\substack{Normal\\Force}}
\end{aligned} \tag{3.30}$$

The above differential equations of motion of the orbital elements are not easily solved, but a good approximation can be made by assuming a constant inclination.

$$\begin{aligned}
i(t) &\approx i_0 - \frac{3\sqrt{\mu}J_2R_e^2}{2\,k\,r^{7/2}} Cos\,i\; Sin\,i\; Sin^2(k\,t) \\
\Omega(t) &\approx \Omega_0 - \frac{3\sqrt{\mu}J_2R_e^2}{2\,k\,r^{7/2}} Cos\,i\; (t\,k - \frac{Sin(2\,k\,t)}{2}) \\
\theta(t) &\approx n\,c\,t + \frac{3\sqrt{\mu}J_2R_e^2}{2\,k\,r^{7/2}} Cos^2 i\; (t\,k - \frac{Sin(2\,k\,t)}{2}) \\
k &= n\,c + \frac{3\sqrt{\mu}J_2R_e^2}{2\,r^{7/2}} Cos^2 i
\end{aligned} \tag{3.31}$$

Equation (3.31) can now be substituted back into equation (3.29) to provide an approximate equation of motion for the reference orbit.

3.4.3 Angular Rotation Rate of the New Reference Orbit

Now that we have modified the reference orbit, the angular velocity $\vec{\omega}$ of the coordinate system must now be calculated again. The angular rate can be defined by

$$\begin{aligned}\vec{\omega} = &(\left(\frac{d\Omega}{dt}\right) Sin\, i\ Sin\,\theta + \left(\frac{di}{dt}\right) Cos\,\theta)\hat{x} \\ &+(\left(\frac{d\Omega}{dt}\right) Sin\, i\ Cos\,\theta - \left(\frac{di}{dt}\right) Sin\,\theta)\hat{y} \\ &+(\left(\frac{d\theta}{dt}\right) + \left(\frac{d\Omega}{dt}\right) Cos\, i)\hat{z}\end{aligned} \tag{3.32}$$

Substituting in equation (3.31) and taking the time average results in

$$\vec{\omega} = c\, n\, \hat{z} \tag{3.33}$$

This is the same angular rate as derived with the previous reference orbit used in the 1st solution. This makes sense because a normal force should not affect the angular rotational rate.

3.4.4 Final Solution – New Reference Orbit – Solution 2

Because we have added a component of the J_2 disturbance to the reference orbit, that component must be subtracted from the equations of motion. The resulting equations of motion are

$$\begin{aligned}&\ddot{\vec{x}} + 2\vec{\omega}\times\dot{\vec{x}} + \dot{\vec{\omega}}\times\vec{x} + \vec{\omega}\times(\vec{\omega}\times\vec{x}) = \\ &\qquad \nabla\vec{g}(\vec{r}_{ref})\cdot\vec{x} + \vec{J}_2(\vec{r}_{ref}) + \frac{1}{2\pi}\int_0^{2\pi}\nabla\vec{J}_2(\vec{r}_{ref})\,d\theta\cdot\vec{x} - \frac{1}{2\pi}\int_0^{2\pi}\vec{J}_2(\vec{r}_{ref})\,d\theta - \vec{J}_2(\vec{r}_{ref})\cdot\hat{N}\end{aligned} \tag{3.34}$$

Substituting the appropriate terms into the equations results in

$$\ddot{x} - 2(n\,c)\,\dot{y} - (5c^2 - 2)n^2 x = -3n^2 J_2 \frac{R_e^2}{r_{ref}}\left(\frac{1}{2} - \frac{3\,Sin^2 i_{ref}\;Sin^2(k\,t)}{2} - \frac{(1+3\,Cos\,2i_{ref})}{8}\right)$$

$$\ddot{y} + 2(n\,c)\,\dot{x} = -3n^2 J_2 \frac{R_e^2}{r_{ref}} Sin^2 i_{ref}\;Sin(k\,t)\,Cos(k\,t) \qquad (3.35)$$

$$\ddot{z} + (3c^2 - 2)\,n^2\,z = 0$$

These can be solved, resulting in

$$x = (x_0 - \alpha_2)\,Cos(n\,t\sqrt{1-s}) + \frac{\sqrt{1-s}}{2\sqrt{1+s}}\,y_0\,Sin(n\,t\sqrt{1-s}) + \alpha_2\,Cos(2\,k\,t)$$

$$y = -\frac{2\sqrt{1+s}}{\sqrt{1-s}}(x_0 - \alpha_2)\;Sin(n\,t\sqrt{1-s}) + y_0\,Cos(n\,t\sqrt{1-s}) + \beta_2\;Sin(2\,k\,t) \qquad (3.36)$$

$$z = z_0\,Cos(n\,t\sqrt{1+3s}) + \frac{\dot{z}_0}{n\sqrt{1+3s}}\,Sin(n\,t\sqrt{1+3s})$$

$$\dot{y}_0 = -2n\sqrt{1+s}\;x_0 + \frac{3n\,J_2 R_e^2}{8k\,r_{ref}}(1 - Cos\,2i) \qquad \dot{x}_0 = y_0\,n\,\left(\frac{1-s}{2\sqrt{1+s}}\right)$$

$$\alpha_2 = -\frac{3\,J_2\,R_e^2\,n^2}{8k\,r_{ref}}\frac{(3k - 2n\sqrt{1+s})}{(n^2(1-s) - 4k^2)}(1 - Cos\,2i)$$

$$\beta_2 = -\frac{3\,J_2\,R_e^2\,n^2}{8k\,r_{ref}}\frac{(2k(2k - 3n\sqrt{1+s}) + n^2(3+5s))}{2\,k(n^2(1-s) - 4k^2)}(1 - Cos\,2i)$$

$$s = \frac{3J_2 R_e^2}{8\,r_{ref}^2}(1 + 3\,Cos\,2i) \qquad k = n\sqrt{1+s} + \frac{3n\,J_2\,R_e^2}{2\,r_{ref}^2}Cos^2 i$$

3.5 Correcting Out of Plane Motion – Solution 3

This next section will address a problem with the linearized equations of motion as derived in the previous section. More specifically, the cross-track motion is not currently modeled correctly. The cross-track motion is deceivingly the most complex motion seen by the satellite cluster. While the linearized differential equations of motion look simple for the $\hat{z}$ direction, (they are not coupled with the other directions), the actual motion is more complex and is not captured by the equations so far.

3.5.1 Why do the linearized equations of motion fail?

Under the influence of the J_2 disturbance force, the orbital planes rotate around the $\hat{Z}$ axis (the north pole). This is due to the fact that the J_2 disturbance force is symmetric across the equator. The new linearized equations of motion, instead of predicting that the orbital planes rotate around the $\hat{Z}$ axis, predict that the orbital planes rotate around the vector normal to the reference orbit. So in the equatorial case, the linearized equations of motion correctly represent the out of plane motion, (the normal vector to the orbital plane points in the same direction as $\hat{Z}$). However, for inclinations other than equatorial, the linearized equations of motion incorrectly model the out of plane motion.

And again the question is why do the linearized equations of motion fail? The reason is that the J_2 disturbance force is modeled by taking the time average of the gradient of the J_2 disturbance force (see section 3.3.5). This assumption causes the J_2 disturbance to appear symmetrical about the current reference orbital plane. Once again, for an equatorial orbit, the time average of the J_2 disturbance is not a simplification since the J_2 disturbance force is always a constant, and symmetrical about the equator.

For in-plane motion, the assumption of the time averaged J_2 disturbance is not a significant error and no changes are required. However for cross-track motion, the error is significant. In this section we will develop a new equation for the out of plane motion based on the geometry of the moving orbital planes. At the same time, the analysis will

be expanded so that differential J_2 effects due to different satellite inclinations will be taken into account.

3.5.2 Description of Cross-Track Motion

Cross-track motion is due solely to the fact that the satellite orbit and the associated reference orbit are not coplanar. It is a periodic motion that is equal to zero when the two orbital planes intersect, and is at a maximum 90° away from the intersection of the planes. The intersection of the two planes is based on differences in the inclination and longitude of the ascending node between the orbital planes. Under the influence of the J_2 disturbance force, these orbital planes move.

As these orbital planes move, both the period and the amplitude of the periodic terms change. This changing is not linear, and spherical trigonometry will be used to derive the out-of-plane motion. Once the period *B(t)* and amplitude *A(t)* are known as functions of time, the equation for out of plane motion can be written in the form

$$z = A(t)\left(\frac{z_0}{A(0)} Cos(B(t)\,t) + \frac{\left(\frac{\dot{z}_0}{n\sqrt{1+3s}} \right)}{A(0)} Sin(B(t)\,t) \right) \tag{3.37}$$

3.5.3 The Period of the Periodic Terms

The period of the periodic terms is defined as the length of time between crossing the intersection of the two planes and returning to that same intersection. When the orbital planes move, the location of this intersection also changes, and thus the period of the periodic terms is also changing. In this section, the distance between the intersections of the orbital planes from one pass to the next will be calculated. Since the velocity of the satellite is known, the resulting period can be determined.

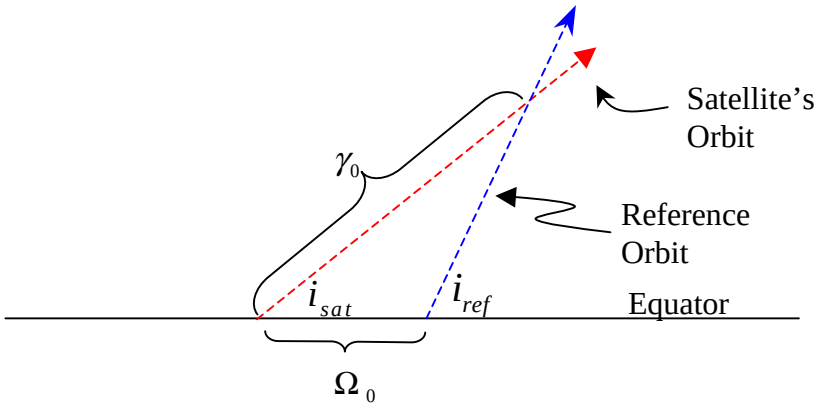

Figure 3-6 : Location of the Intersection of the Two Orbital Planes

Figure 3-6 shows the orbit of a reference orbit, and the orbit of the satellite as they cross the equator. i_{ref} and i_{sat} are the inclination of the reference orbit and the satellite respectively. Ω_0 is the initial angular separation of the longitude of the ascending node between the two orbits. γ_0 is the angular distance from the satellite's equatorial crossing, and the crossing of the two orbits. γ_0 can be calculated using spherical trigonometry.

$$\gamma_0 = Cot^{-1}\left(\frac{Cos\, i_{sat}\ Cos\,\Omega_0 - Cot\, i_{ref}\ Sin\, i_{sat}}{Sin\,\Omega_0}\right) \tag{3.38}$$

Because of the J_2 disturbance force, the orbits' longitude of the ascending node will precess. This precession of the two orbital planes causes the location of the crossing of the two orbital planes to change. The extra distance that the satellite must travel before crossing the reference orbit can be calculated using Figure 3-7.

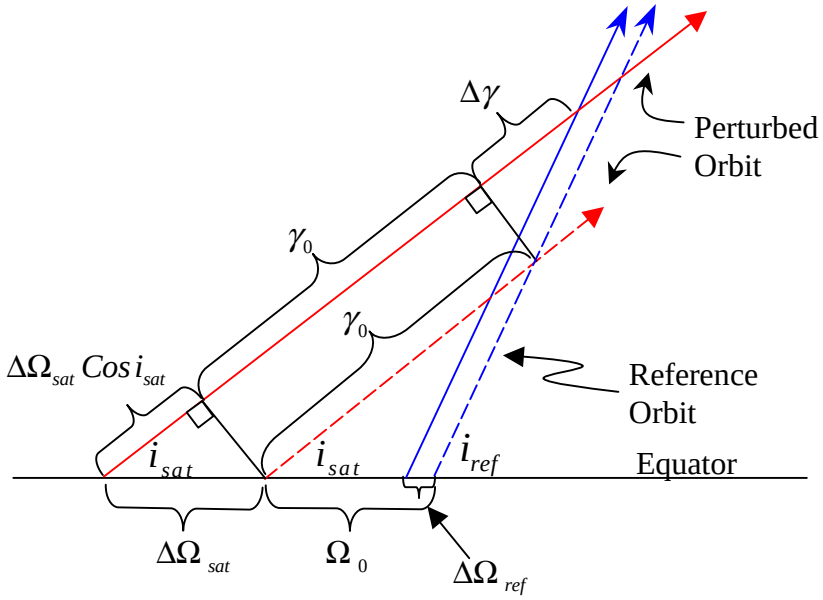

Figure 3-7 : The Moving Intersection of the Orbital Planes

Figure 3-7 shows the changing location of the orbital plane crossing. The dashed line represents the initial orbital plane, while the solid line is the orbital plane at a later time. The location of the orbital plane crossing can be described by a change in the distance between the satellites equatorial crossing and the crossing of the reference orbit $\Delta\gamma$.

$$\Delta\gamma = Cot^{-1}\left(\frac{Cos\,i_{sat}\;Cos\,\Omega_{net} - Cot\,i_{ref}\;Sin\,i_{sat}}{Sin\;\Omega_{net}}\right) - \Delta\Omega_{sat}\,Cos\,i_{sat} - \gamma_0 \qquad (3.39)$$

$$\begin{aligned}
\Omega_{net} &= \Omega_0 + \Delta\Omega_{sat} - \Delta\Omega_{ref} \\
\Delta\Omega_{sat} &\approx -\frac{3}{2}\frac{J_2\,n\,R_e^2\,t}{r_{ref}^{\;2}}Cos\,i_{sat} \qquad (3.40) \\
\Delta\Omega_{ref} &\approx -\frac{3}{2}\frac{J_2\,n\,R_e^2\,t}{r_{ref}^{\;2}}Cos\,i_{ref}
\end{aligned}$$

Equation (3.39) determines the extra distance that the satellite must travel ($\Delta\gamma$) as a function of time. While this solution provides an accurate means of determining this

distance, it is a little tedious to calculate. A first order approximation can be made by calculating the derivative of γ with respect to Ω.

$$\frac{d\gamma}{d\Omega} = \left(\frac{Sin\, i_{ref}\, (Cos\, i_{ref}\ Sin\, i_{sat}\ Cos\, \Omega_0 - Cos\, i_{sat}\ Sin\, i_{ref})}{(Cos\, i_{ref}\ Sin\, i_{sat} - Cos\, i_{sat}\ Sin\, i_{ref}\ Cos\, \Omega_0)^2 + (Sin\, i_{ref}\ Sin\, \Omega_0)^2} \right) \tag{3.41}$$

From this equation, $\Delta\gamma$ can be calculated as

$$\Delta\gamma = \frac{d\gamma}{d\Omega} \Delta\Omega_{net} - \Delta\Omega_{sat}\, Cos\, i_{sat} \tag{3.42}$$

Which is a linear function in time, and can be written as

$$\Delta\gamma = b\, t \tag{3.43}$$

where *b* is a constant.

Both methods provide roughly the same solution. While equation (3.39) is more exact, equation (3.42) is easier to implement once the derivative has been calculated.

Equation (3.42) also allows for some insight into the motion of the location of the orbital plane crossing. When the difference between i_{ref} and i_{sat} is small, and Ω_0 is small, $d\gamma/d\Omega$ becomes very large. Thus small changes in $\Delta\Omega_{net}$ can result in large changes in $\Delta\gamma$. This is due to the relative orientation of the orbital planes and the axis about which they rotate.

This motion can be thought of as a scissoring effect. When a pair of scissors is opened, the point of intersection of the two blades moves very rapidly from the tips back. As the handle is opened further, the rate at which the intersection of the two blades moves towards the handles slows down. With orbital planes, the location of the intersection of the orbital planes will move very quickly away from the equator, and then as it approaches the poles it will slow down.

Once a function for $\Delta\gamma$ has been calculated, the arguments of the periodic terms can be calculated.

$$B(t) = nc - \frac{\Delta\gamma}{t} \tag{3.44}$$

If the first order approximation of $\Delta\gamma$, equation (3.41) and (3.42), is used to calculate $\Delta\gamma$ then *B(t)* is a constant.

$$B(t) = nc - b \tag{3.45}$$

Also, if the orbital planes have no differential movement and the same inclination, $\Delta\Omega_{net} = 0$ and $i_{ref} = i_{sat}$, then

$$\begin{aligned} B(t) &= n\,c - b = k \\ k &= n\,c + \frac{3n\,J_2\,R_e^2}{2\,r_{ref}^2} Cos^2 i \end{aligned} \tag{3.46}$$

3.5.4 Amplitude

The amplitude of the out-of-plane terms is dependent on the maximum separation between the two different orbital planes. This can once again be calculated with spherical trigonometry.

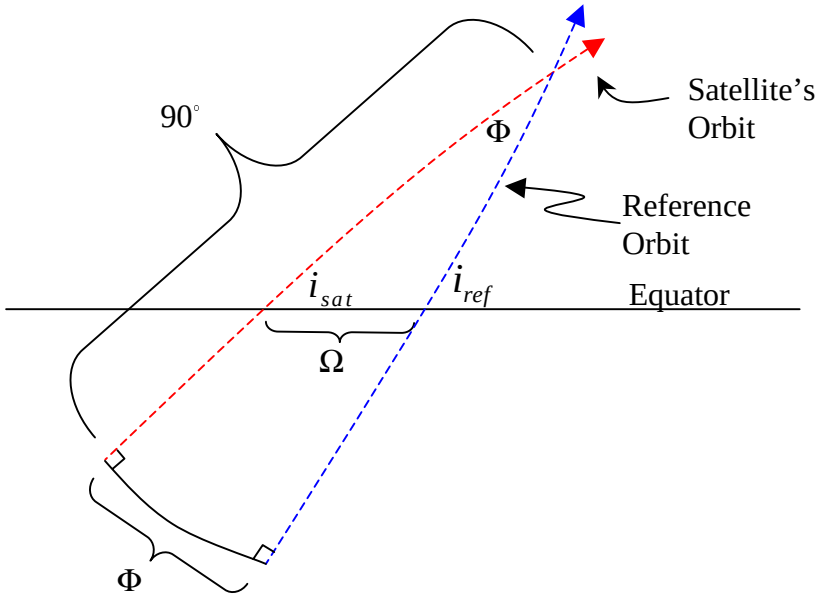

Figure 3-8 : Determining the Amplitude

From Figure 3-8, it can be seen that the maximum amplitude is based only on the inclination of both orbits, and their separation at the equator.

The angle Φ can be calculated using

$$\Phi(t) = Cos^{-1}\left(Cos\, i_{sat}\ Cos\, i_{ref} + Sin\, i_{sat}\ Sin\, i_{ref}\ Cos\,\Omega(t)\right) \tag{3.47}$$

where Ω is the time varying separation of the longitude of the ascending nodes.

Now that Φ has been determined as a function of time, the amplitude of the out of plane motion can be defined as

$$A(t) = r_{ref}\ \Phi(t) = r_{ref}\ Cos^{-1}\left(Cos\, i_{sat}\ Cos\, i_{ref} + Sin\, i_{sat}\ Sin\, i_{ref}\ Cos\,\Omega(t)\right) \tag{3.48}$$

There are times when the inclination of the reference orbit and the inclination of the satellite are identical. When this is the case, the two orbital planes intersect at $\theta = 90^{\circ}$, and using Figure 3-9 the amplitude can be more simply calculated by

$$\Phi(t) = 2Sin^{-1}(Sin\, i\ Sin\frac{\Omega(t)}{2}) \tag{3.49}$$

When Ω is small, this can be approximated by

$$\Phi(t) \approx \Omega(t)\ Sin\ i \tag{3.50}$$

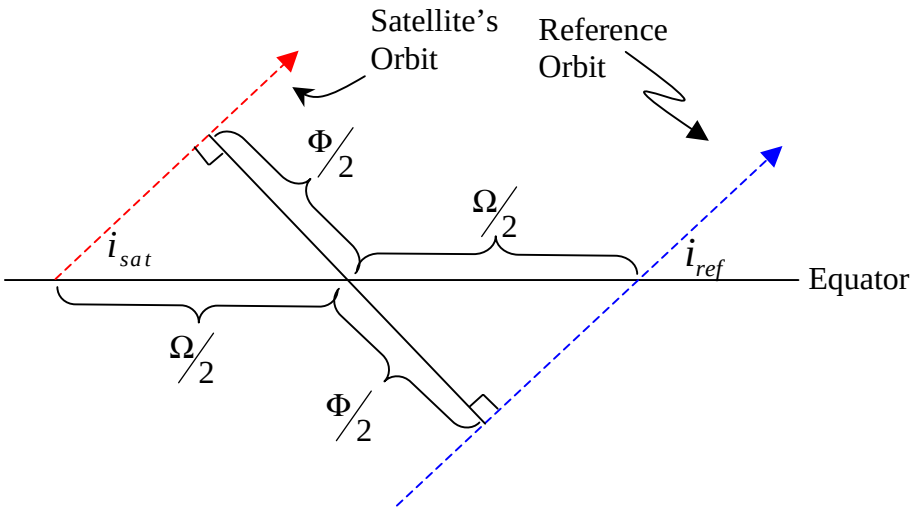

Figure 3-9 : Determining the Amplitude when $i_{ref} = i_{sat}$

3.5.5 Final Out-of-Plane Motion

We can now write the out-of-plane motion as

$$z = A(t)\left(\frac{z_0}{A(0)} Cos(B(t)\,t) + \frac{\left(\frac{\dot{z}_0}{n\sqrt{1+3s}} \right)}{A(0)} Sin(B(t)\,t) \right)$$
$$A(t) = r_{ref}\Phi(t) \tag{3.51}$$
$$B(t) = nc - \frac{\Delta\gamma}{t}$$

When differential motion is not taken into account, there is no change in the amplitude of the cross track terms ($A(t)$ is a constant). $B(t)$ is also a constant. The equations of motion greatly simplify producing

$$z = z_0\, Cos(k\,t) + \frac{\dot{z}_0}{n\sqrt{1+3s}} Sin(k\,t) \tag{3.52}$$

3.6 Relative Motion

While the motion of a satellite with respect to the reference orbit is interesting, what really matters in formation flying is the relative motion of one satellite with respect to another satellite in the cluster.

The equations of motion that describe differential motion can be obtained in two different ways. First, the motion of each satellite can be calculated using the above equations of absolute motion for each satellite. Then this motion is subtracted from one another to produce the relative motion. Otherwise, the equations of motion can be derived by creating a set of differential equations again. Both methods will produce the same results, but the latter is shown here.

Deriving the relative motion can be accomplished by applying the substitution of

$$\vec{x}_2 - \vec{x}_1 = \Delta\vec{x} \tag{3.53}$$

into equation (3.34). $\vec{x}_2$ and $\vec{x}_1$ are the relative positions of two satellites in the cluster.

$$\Delta\ddot{\vec{x}} + 2\vec{\omega}\times\Delta\dot{\vec{x}} + \dot{\vec{\omega}}\times\vec{x} + \vec{\omega}\times(\vec{\omega}\times\Delta\vec{x}) = \nabla\vec{g}(\vec{r}_{ref})\cdot\Delta\vec{x} + \frac{1}{2\pi}\int_0^{2\pi}\nabla\vec{J}_2(\vec{r}_{ref})\,d\theta\cdot\Delta\vec{x} \quad (3.54)$$

3.6.1 Final Relative Motion Equations – No Cross-Track Corrections

Substituting in the appropriate terms results in the following differential equations of motion in $\hat{x}-\hat{y}-\hat{z}$ coordinates

$$\begin{aligned} \ddot{x} - 2(nc)\dot{y} - (5c^2-2)n^2x = 0 \\ \ddot{y} + 2(nc)\dot{x} = 0 \\ \ddot{z} + (3c^2-2)\,n^2z = 0 \end{aligned} \quad (3.55)$$

It should be noted that this is just the homogenous solution to the equations derived in the 1st and 2nd solutions above.

Solving the differential equations results in

$$\begin{aligned} x &= x_0 Cos(\sqrt{1-s}\,nt) + \frac{\sqrt{1-s}}{2\sqrt{1+s}}\,y_0\,Sin(\sqrt{1-s}\,nt) \\ y &= -\frac{2\sqrt{1+s}}{\sqrt{1-s}}\,x_0\,Sin(\sqrt{1-s}\,nt) + y_0 Cos(\sqrt{1-s}\,nt) \\ z &= z_0 Cos(n\sqrt{1+3s}\,t) + \frac{\dot{z}_0}{n\sqrt{1+3s}}\,Sin(n\sqrt{1+3s}\,t) \\ \dot{x}_0 &= \frac{n\,y_0}{2}\frac{(1-s)}{\sqrt{1+s}} \qquad \dot{y}_0 = -2\,n\,x_0\sqrt{1+s} \end{aligned} \quad (3.56)$$

where

$$s = \frac{3J_2R_e^2}{8r_{ref}^{\,2}}(1+3\,Cos\,2i_{ref}) \qquad n = \sqrt{\frac{\mu}{r_{ref}^3}}$$

3.6.2 Final Relative Motion Equations – With Cross-Track Corrections

The relative cross-track motion can now be corrected just like the absolute motion equations were in section 3.5. The resulting equations of motion are

$$x = x_0 Cos(\sqrt{1-s}\, n\, t) + \frac{\sqrt{1-s}}{2\sqrt{1+s}}\, y_0\, Sin(\sqrt{1-s}\, n\, t)$$

$$y = -\frac{2\sqrt{1+s}}{\sqrt{1-s}}\, x_0\, Sin(\sqrt{1-s}\, n\, t) + y_0 Cos(\sqrt{1-s}\, n\, t)$$

$$z = A(t)\left(\frac{z_0}{A(0)} Cos(B(t)\, t) + \frac{\left(\frac{\dot{z}_0}{n\sqrt{1+3s}}\right)}{A(0)} Sin(B(t)\, t) \right)$$

$$\dot{x}_0 = \frac{n\, y_0}{2}\frac{(1-s)}{\sqrt{1+s}} \qquad \dot{y}_0 = -2\, n\, x_0 \sqrt{1+s}$$

where

$$s = \frac{3 J_2 R_e^2}{8 r_{ref}^{\ 2}}(1 + 3\, Cos\, 2 i_{ref})$$

$$A(t) = r_{ref}\Phi(t)$$

$$B(t) = nc - \frac{\Delta\gamma}{t} \qquad (3.57)$$

3.7 Initial Conditions and Closed Form Solutions

The solution to the new linearized equations of motion is dependent on six initial conditions. These initial conditions are specified as the initial position and velocity of the satellite ($x_0, y_0, z_0, \dot{x}_0, \dot{y}_0, \dot{z}_0$). However, two of the initial conditions ($\dot{x}_0$ & $\dot{y}_0$) can be solved for to eliminate drift and offset. These initial conditions for ($\dot{x}_0$ & $\dot{y}_0$) have always been calculated and specified in the above solutions for all of the linearized equations of motion.

However, the initial conditions specified by the linearized equations of motion have errors. Because of this, some offset and drift errors are produced. The most common drift

observed is in the $\hat{y}$ direction. This drift signifies a mismatch between the orbital period of the reference orbit and that of the satellite.

The initial conditions given by the new linearized equations of motion do a very good job of predicting the appropriate initial conditions to match the periods. However, they are not exactly right. It turns out that drift in the $\hat{y}$ direction is extremely sensitive to $\dot{y}_0$. Because of this, an error on the order of a few meters per orbit is generated when using the initial conditions specified by the new linearized equations of motion.

New initial conditions can be calculated that will produce closed form solutions. This is done either numerically or analytically. In this section, an analytical method of calculating the appropriate initial conditions is presented for satellites in the same orbital plane. Using these new initial conditions completely removes any drift in the $\hat{y}$ direction.

3.7.1 Why is there an error in the linearized equations initial conditions?

As stated above, the new linearized equations provide for initial starting conditions. These initial conditions are very close to being exact, but there is still error. The reason for this error has two parts. The first is the linearization of the gravity terms. Since these are linearized equations, they do not model the exact gravitational force, but instead a linearized version. Second, when calculating the gradient of the J_2 term, the new linearized equations use the time average of the J_2 force calculated at the radius of the reference satellite, and not the actual force. These two simplifications to the gravitational force are responsible for the small error in predicting the appropriate initial conditions.

3.7.2 Orbital Energy and Period

The period of an orbit is based on the orbit's energy. Satellites with the same energy orbit and the same inclination, have the same period. Total energy is the sum of a satellite's potential and kinetic energy.

$$E = K.E. + P.E. \tag{3.58}$$

Once the total energy the orbit is calculated the velocity can be found.

3.7.3 The Total Energy of the Orbit

The total energy of the satellite's orbit can be found by calculating the total energy of the reference orbit. The specific kinetic energy of the reference orbit is given as

$$K.E. = \frac{v^2}{2} = \frac{(\omega' r_{ref})^2}{2} = \frac{(n\sqrt{1+s}\, r_{ref})^2}{2} = \frac{\mu}{r_{ref}} \frac{1+s}{2} \tag{3.59}$$

Because the reference orbit is considered to be under the influence of an averaged J_2 disturbance, the average of the potential energy is used to calculate its gravitational potential.

$$P.E. = -\frac{\mu}{r_{ref}}(1 + \frac{J_2 R_e^2}{8 r_{ref}^2}(1 + 3Cos\, 2i_{sat})) \tag{3.60}$$

Thus the total energy of the orbit is given as

$$\begin{aligned} E &= \frac{\mu}{r_{ref}} \frac{1+s}{2} - \frac{\mu}{r_{ref}}(1 + \frac{J_2 R_e^2}{8 r_{ref}^2}(1 + 3Cos\, 2i_{sat})) \\ E &\approx -\frac{\mu}{r_{ref}}(\frac{1}{2} - \frac{s}{6}) \end{aligned} \tag{3.61}$$

3.7.4 Determining the Velocity of the Perturbed Satellite

The satellite's specific kinetic energy is given as

$$K.E. = \frac{v_{In-Plane}^2}{2} \tag{3.62}$$

And the satellite's specific potential energy is given as

$$P.E. = -\frac{\mu}{r_{sat}}\left(1 - \frac{J_2 R_e^2}{r_{sat}^2}\left(\frac{3Sin^2\theta_{sat}\ Sin^2 i_{sat} - 1}{2}\right)\right) \tag{3.63}$$

Equation (3.62) and (3.63), along with (3.61), can be substituted into (3.58) resulting in

$$-\frac{\mu}{r_{ref}}\left(\frac{1}{2} - \frac{s}{6}\right) = \frac{v_{In-Plane}^2}{2} - \frac{\mu}{r_{sat}}\left(1 - \frac{J_2 R_e^2}{r_{sat}^2}\left(\frac{3Sin^2\theta_{sat}\ Sin^2 i_{sat} - 1}{2}\right)\right) \tag{3.64}$$

By solving the above equation, the speed of the satellite in inertial space can be determined.

$$v_{In-Plane} = \sqrt{\frac{2\mu}{r} + \frac{J_2 R_e^2 \mu(1 - 3Sin^2 i\ Sin^2\theta)}{r^3} - \frac{(1 - \frac{s}{3})\mu}{r_{ref}}} \tag{3.65}$$

3.7.5 Direction and Relative Speed

One the inertial velocity of the satellite is known (whether through the steps outlined above or by other numerical methods), the direction and relative speed must now be calculated. Assuming that the error in the initial velocity conditions comes from the $\hat{y}$ direction,

$$v_{In-Track} = \sqrt{v_{In-Plane}^2 - \dot{x}_0^2} \tag{3.66}$$

The relative velocity can be calculated by

$$\dot{y}_0 = v_{in-track} - v_{ref} - n c x_0 \tag{3.67}$$

where v_{ref} is the velocity of the reference orbit in inertial space, and $n c x_0$ is due to the rotating reference frame.

3.7.6 Closed Form Solutions Conclusions

The initial conditions given by the equations of motion are very close, but the small errors eventually cause a drift in the in-track direction. In this section a method of calculating the correct initial velocity is presented. However, this method only works for satellites in similar inclinations. For satellites in different inclinations, the period will be different even though both satellites have the same orbital energy. Another method must be utilized to calculate the initial conditions for zero drift.

3.8 Detailed Derivation Conclusions

In this chapter, we have derived a new set of linearized equations of motion for satellite clusters. As we stepped through the derivation process, three different absolute motion solutions were developed. In the first solution, a circular orbit with a modified period was used, but the satellite and the reference orbit still drifted apart due to drift in the longitude of the ascending node. Because of this, the second solution was developed which used a new reference orbit. This reference orbit incorporated the normal component of the J_2 disturbance into its own equations of motion. However, the equation of motion of the reference orbit can no longer be analytically derived. An approximation is developed and presented using variations in the orbital elements.

In the derivation of the final solution, the cross-track motion was examined. It was determined that the cross-track motion was not being modeled correctly. Because of this error, a new solution was developed based on the mean variations of the longitude of the ascending node, and the geometric properties between the two orbital planes.

Relative motion was then considered. While the motion of a satellite with respect to a known reference orbit is needed, the relative motion between spacecraft is more important. The equations of motion for this relative motion were derived in the same way the absolute solutions were. However, the solution could have been calculated by just subtracting the absolute motion of the two spacecraft. The cross-track motion correction was also applied to these relative motion equations. It should be noted that this cross-track motion captures the differential J_2 effects.

Finally, the error in the initial conditions is discussed, and a method of calculating the correct initial conditions is presented for satellites in the same orbital plane. For satellites having different inclinations, a different method, not discussed in this thesis, must be used.

In the next chapter, the solutions to these new linearized differential equations of motion will be compared to a numerical simulator to check for validity. It will be shown that the equations developed here do a very good job of modeling the J_2 disturbance force, and will be a good replacement for Hill's equations for satellite formation flying.

Chapter 4

VERIFFICATION OF THE NEW LINEARIZED EQUATIONS OF MOTION

In chapter 4, the solutions to the new linearized equations of motion will be checked for validity. This will be done in two ways. The first method will be to compare the solutions derived in chapter 3 to the mean variation of the orbital elements due to the J_2 disturbance. Then the solutions will be compared to a numerical simulator.

4.1 Comparison of the Solution with the Mean Variation of the Orbital Elements

The new linearized equations of motion are now checked for validity by comparing the solution to the linearized equations with the mean variation in the orbital elements due to the J_2 disturbance.

Under the influence of the J_2 disturbance, each of the satellite's orbital elements, (semi-major axis, eccentricity, inclination, longitude of the ascending node, argument of periapsis, and true anomaly), undergoes changes. Effects due to these changes will be observed in the solution to the new linearized equations of motion.

The variations of the orbital elements averaged over one period were derived using first principles in [3] and are used here to validate the linearized equations of motion. A summary of these variations is shown below in equation (4.1).

$$\left(\frac{\partial a}{\partial \theta}\right)_{Avg} = 0 \quad \left(\frac{\partial e}{\partial \theta}\right)_{Avg} = 0 \quad \left(\frac{\partial i}{\partial \theta}\right)_{Avg} = 0$$
$$\left(\frac{\partial \Omega}{\partial \theta}\right)_{Avg} \approx -\frac{3J_2 R_E^2}{2r^2} Cos[i]$$
$$\left(\frac{\partial \omega}{\partial \theta}\right)_{Avg} \approx -\left(\frac{\partial \Omega}{\partial \theta}\right)_{Avg} Cos[i] + \frac{3J_2 R_E^2}{8r^2}(1 + 3Cos[2i]) \tag{4.1}$$
$$\left(\frac{\partial M}{\partial t}\right)_{Avg} \approx n_{J_2} + n\left(\frac{\partial \omega}{\partial \theta}\right)_{Avg}$$

4.1.1 Semi-major Axis

$$\left(\frac{\partial a}{\partial \theta}\right)_{Avg} = 0 \tag{4.2}$$

The presence of the J_2 term has no effect on the mean variation of the semi major axis. A variation in the semi-major axis would manifest itself in the solution to the linearized equations of motion as a secular drift term in the $\hat{x}$ direction. Since the solution to the linearized equations of motion has no such term, it is in agreement with the mean variation of the semi-major axis.

4.1.2 Eccentricity

$$\left(\frac{\partial e}{\partial \theta}\right)_{Avg} = 0 \tag{4.3}$$

The J_2 disturbance force has no effect on the mean variation of the eccentricity. A variation in the eccentricity would manifest itself in the solution to the linearized equations of motion as an increase in the amplitude of the periodic terms in the $\hat{x}$ direction. Since the amplitude of the periodic terms is constant, the solution is once again in agreement with the mean variation of the orbital elements.

4.1.3 Inclination

$$\left(\frac{\partial i}{\partial \theta}\right)_{Avg} = 0 \tag{4.4}$$

The J_2 disturbance has no effect on the mean variation of the inclination of an orbit. A variation in the inclination would be manifested as a combination of many different components of the solution. These include the period of the $\hat{z}$ term, the magnitude of the periodic terms in the $\hat{z}$ equation, and the initial conditions. As discussed in section 3.5, the first two solutions to the linearized equations of motion do not properly capture this cross-track motion. However, because the 3rd solution is based on the constant inclination of the satellite, this variation is captured in the 3rd solution.

4.1.4 Ascending Node

$$\left(\frac{\partial \Omega}{\partial \theta}\right)_{Avg} \approx -\frac{3J_2R_e^2}{2r^2}Cos\, i \tag{4.5}$$

The J_2 disturbance does have an effect on the mean variation in the longitude of the ascending node. A variation in the longitude of the ascending node would manifest itself as a change in the amplitude of the periodic terms in the $\hat{z}$ direction.

It is interesting to note that the 1st solution does a very good job of capturing the change in the longitude of the ascending node and will be looked at in more depth here.

When the reference orbit and the perturbed satellite's orbit have the same inclination, the relationship between the variation in the longitude of the ascending node and the $\hat{z}$ terms is shown in Figure 4-1. If both the satellite and the reference orbit start at point A, after one orbital period the reference orbit will return to point A, and the perturbed satellite will end up at point B.

This relationship is

$$\Delta z = r\, \Delta\Omega\, Sin\, i \tag{4.6}$$

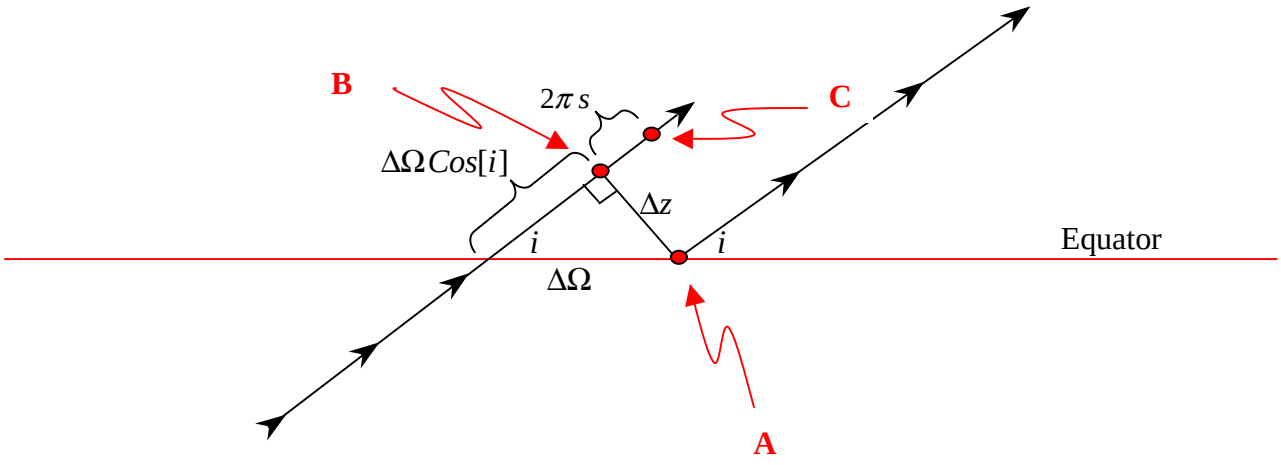

Figure 4-1 : Variation in the Longitude of the Ascending Node

From equation (3.27), the motion in the $\hat{z}$ direction is given as

$$z = z_0\, Cos(n t\sqrt{1+3s}) + \frac{\dot{z}_0}{n\sqrt{1+3s}} Sin(n t\sqrt{1+3s}) + \beta(\sqrt{1+s}\ Sin(n t\sqrt{1+3s}) - \sqrt{1+3s}\, Sin(n t\sqrt{1+s})) \tag{4.7}$$

It is the 2nd half of the equation that is responsible for the variation of the ascending node.

$$\Delta z = \beta(\sqrt{1+s}\ Sin(n t\sqrt{1+3s}) - \sqrt{1+3s}\, Sin(n t\sqrt{1+s})) \tag{4.8}$$

This term is the combination of two periodic terms with a small difference in their period. The resulting function is a periodic term with increasing amplitude. The envelope that contains this function is given by

$$\Delta\tilde{z} = \beta\,(\sqrt{1+s} + \sqrt{1+3s})\, Sin[n t \frac{(\sqrt{1+s} - \sqrt{1+3s})}{2}] \tag{4.9}$$

Taking the derivative with respect to time and simplifying

$$\begin{aligned}
\dot{\tilde{z}} &= \beta\,(n\,s)\,Cos\,(n\,t\,\frac{(\sqrt{1+s}-\sqrt{1+3s})}{2}) \\
\dot{\tilde{z}} &= \frac{3}{2}\frac{n\,J_2\,R_e^2}{r\sqrt{1+3s}}\,Cos\,i\;Sin\,i\,Cos\,(n\,t\,\frac{(\sqrt{1+s}-\sqrt{1+3s})}{2}) \\
\dot{\tilde{z}} &= \frac{1}{\sqrt{1+3s}}\,(r\,\dot{\Omega}\,Sin\,i) \quad \text{at} \quad t=0 \\
\dot{\tilde{z}} &\approx (r\,\dot{\Omega}\,Sin\,i) \quad \text{at} \quad t=0
\end{aligned} \tag{4.10}$$

As shown above, the solution does capture the precession of the longitude of the ascending node. There is only a small discrepancy in the additional $1/\sqrt{1+3s}$ term.

For the 3rd solution of the absolute motion, and for the relative motion, changes in the longitude of the ascending node were discussed in depth in section 3.5. The variation in the longitude of the ascending node was used to derive the cross-track motion, and thus the mean variation in the longitude of the ascending node is captured by the new linearized equations of motion.

4.1.5 Argument of Periapsis

$$\begin{aligned}
\left(\frac{\partial\omega}{\partial\theta}\right)_{Avg} &= -\left(\frac{\partial\Omega}{\partial\theta}\right)_{Avg} Cos[i] + \frac{3J_2R_E^2}{8r^2}(1+3Cos[2i]) \\
\left(\frac{\partial\omega}{\partial\theta}\right)_{Avg} &= -\left(\frac{\partial\Omega}{\partial\theta}\right)_{Avg} Cos[i] + s
\end{aligned} \tag{4.11}$$

The variation in the argument of periapsis has two components. The first component is a geometric effect due to the movement of the longitude of the ascending node. Once again referring to Figure 4-1, after one orbital period the perturbed satellite and the argument of periapsis will be at point B due to the variation in the longitude of the ascending node. This is the first term in the variation of the argument of periapsis. The second component is directly an effect from the J_2 disturbance. After one orbital period the argument of periapsis also moves an additional amount $2\pi\,s$, and ends up at point C.

The first term is due to the variation in the longitude of the ascending node and has already been verified.

The second term is represented in the new linearized equations of motion by the difference in periods between the $\hat{x}$ and $\hat{y}$ terms and the reference orbit. The argument of periapsis is the point of closest approach for the satellite. When periapsis drifts, the point of closest approach is earlier or later in the orbit. At the point of closest approach, the periodic terms in the $\hat{x}$ and $\hat{y}$ equations are at a minimum. So, as the argument of periapsis move, so must the time of the minima. Therefore, the motion of the argument of periapsis is represented in the difference between the periods of the *x* and *y* terms, and the orbital period.

Shown below is the reference orbit's orbital period, and the period of the periodic terms in the *x* and *y* directions.

$$\begin{aligned} P_{ref} &= \frac{2\pi}{n\sqrt{1+s}} \approx (1-\frac{s}{2})\frac{2\pi}{n} \\ P_{x/y} &= \frac{2\pi}{n\sqrt{1-s}} \approx (1+\frac{s}{2})\frac{2\pi}{n} \end{aligned} \tag{4.12}$$

The difference between these two periods is the amount that the argument of periapsis has moved.

$$P_{x/y} - P_{ref} = s\frac{2\pi}{n} \tag{4.13}$$

Which corresponds to a differential angular rate of s which is the second term in the variation of the longitude of the ascending node. The movement of the argument of periapsis is therefore captured by the linearized equations.

4.1.6 Mean Anomaly

$$\left(\frac{\partial M}{\partial t}\right)_{Avg} \approx n_{J_2} + n\left(\frac{\partial \omega}{\partial \theta}\right)_{Avg} \tag{4.14}$$

A variation of the mean anomaly causes a change in the period of the orbit. This change in the orbital period was captured by the new linearized equations by "speeding up" the reference orbit to match the period of the perturbed satellites.

4.1.7 Conclusion

In this section, it was shown that the new linearized equations of motion are able to capture all aspects of the mean motion of a satellite under the J_2 disturbance force. This was accomplished by calculating the mean variation of each orbital element and observing the associated changes in the solution to the linearized equations of motion.

4.2 Numerical Comparison Overview

In the following sections, the solutions to the new linearized equations of motion will be compared to a numerical simulation. These results will be used to verify that the new linearized equations of motion are capturing the effect of the J_2 disturbance force. Hill's equations will be used as a benchmark for comparison.

There are six different initial conditions that can be specified. Three position components (x_o, y_o, z_o), and three velocity components $(\dot{x}_o, \dot{y}_o, \dot{z}_o)$. However, for zero-offset and zero-drift conditions, two of the initial velocity components $(\dot{x}_o, \dot{y}_o)$ can be solved for.

In each simulation, the closed form of the solution will be used. In other words, the initial conditions $(\dot{x}_o, \dot{y}_o)$ will be set according to the linearized equations of motion to prevent any type of drift or average offset. These initial velocities vary depending on the specific linearized equations used.

For these numerical simulations, a cluster with a semi-major axis of 7000 km, inclination of 35°, and an inter-satellite spacing of 100 m is used.

The results for each simulation will be presented in a similar method. Each figure will have six different plots. Along the left side will be the motion of the satellite in the three orthogonal directions (radial, in-track, and cross-track). Each plot will have the motion of the satellite according to the linearized equations of motion (solid line), and the motion as determined from a numerical simulation (dashed line). Along the right side of the figure will be the differences between the numerical simulation and the solution to the linearized equations of motion.

4.2.1 Types of Errors

Because the new equations of motion are approximate solutions, there will be errors. These errors will generally be combination of three types of errors: periodic, periodic with increasing amplitude, and secular errors.

4.2.1.1 Periodic errors

Throughout the simulation, periodic errors will always be present. The errors will have many different sources. Periodic errors on the order of centimeters are due to the limitations of the new linearized equations of motion. Because the equations are linearized and time averaged, they do not capture the higher order effects of the J_2 disturbance. These effects manifest themselves as small periodic errors.

4.2.1.2 Periodic with increasing amplitude

The second type of error is periodic with increasing amplitude. There are two different reasons for this. First, the motion in all three orthogonal directions is usually periodic. When the linearized equations predict motion with a different period than the numerical simulation, a periodic error with increasing amplitude occurs.

The second reason why there could be a periodic error with increasing amplitude is that the actual motion is periodic with increasing amplitude, and the linearized equations of

motion don't capture the effect. This occurs when the satellite and the reference orbit have different variations of the longitude of the ascending node. The amplitude of the out-of-plane motion increases with time. When the linearized equations of motion do not capture this effect correctly, an increasing periodic error appears.

4.2.1.3 Secular drift

The third type of error is secular. This error is only manifested in the in-track direction and is a direct result of a difference in orbital periods. When the orbital periods of the reference satellite and the actual satellite are different, they drift apart in the in-track direction. Since the linearized equations will be in the closed-form solution, they will predict no drift. When this drift does happen, there is a secular error in the in-track direction.

4.3 Absolute Motion — Zero Initial Conditions

In this section we will look at the absolute motion of the satellite cluster. The origin of the cluster can really be specified with any initial conditions, but this simulation will use 'zero' initial conditions. The satellite and the reference orbit will have the same position, though not necessarily the same velocity, at the beginning of the simulation.

The solution to Hill's equations will be presented first and used as a baseline. This will show the improvement the new linearized equations of motion have over Hill's equations. Both the 1st and 2nd solution derived in chapter 3 will be presented in this section. The 3rd solution where the cross-track motion is corrected is not presented because there is no cross-track motion. Since both the satellite and the reference orbit will have the same inclination, the 3rd solution reduces to the 2nd solution in that case.

4.3.1 Hill's Equations

In Hill's equations, the reference orbit is an unperturbed circular orbit with the following parameters

$$\begin{aligned} r_{ref} &= 7000 \text{ km} \\ i_{ref} &= 35^{\circ} \\ \omega_f &= n = 0.00107801 \text{ 1/sec} \end{aligned} \tag{4.15}$$

Hill's equations are given as

$$\begin{aligned} x &= x_0\, Cos(n\,t) + \frac{1}{2} y_0\, Sin(n\,t) \\ y &= -2\, x_0\, Sin(n\,t) + y_0\, Cos(n\,t) \\ z &= z_0\, Cos(n\,t) + \frac{\dot{z}_0}{n} Sin(n\,t) \\ \dot{y}_0 &= -2n\, x_0 \qquad \dot{x}_0 = \frac{1}{2} n\, y_0 \end{aligned} \tag{4.16}$$

Using the 'zero' initial conditions, the position and velocity of the satellite are identical to the position and velocity of the reference satellite. Because of this, the initial relative states are zero.

$$\begin{aligned} x_0 &= 0 \quad \dot{x}_0 = \frac{n\, y_0}{2} = 0 \\ y_0 &= 0 \quad \dot{y}_0 = -2\, n\, x_0 = 0 \\ z_0 &= 0 \quad \dot{z}_0 = 0 \end{aligned} \tag{4.17}$$

Substituting the initial conditions (equation (4.17)) into the equations of motion (equation (4.16)), the following equations of motion are created

$$\begin{aligned} x &= 0 \\ y &= 0 \\ z &= 0 \end{aligned} \tag{4.18}$$

Essentially Hill's equations state that the origin of the cluster will remain at the exact same position as the reference satellite. When there are no disturbance forces, this is a correct assumption. However, under the J_2 disturbance this is no longer true. Figure 4-2 shows the actual motion of the origin cluster compared to motion specified by Hill's equations.

Shown below are the results from the numerical simulation. The plots on the left show the motion of the cluster origin in three directions. The dashed plot is the numerical simulation, while the solid line is the solution to the linearized equations. Directly to the right is the difference between the two solutions.

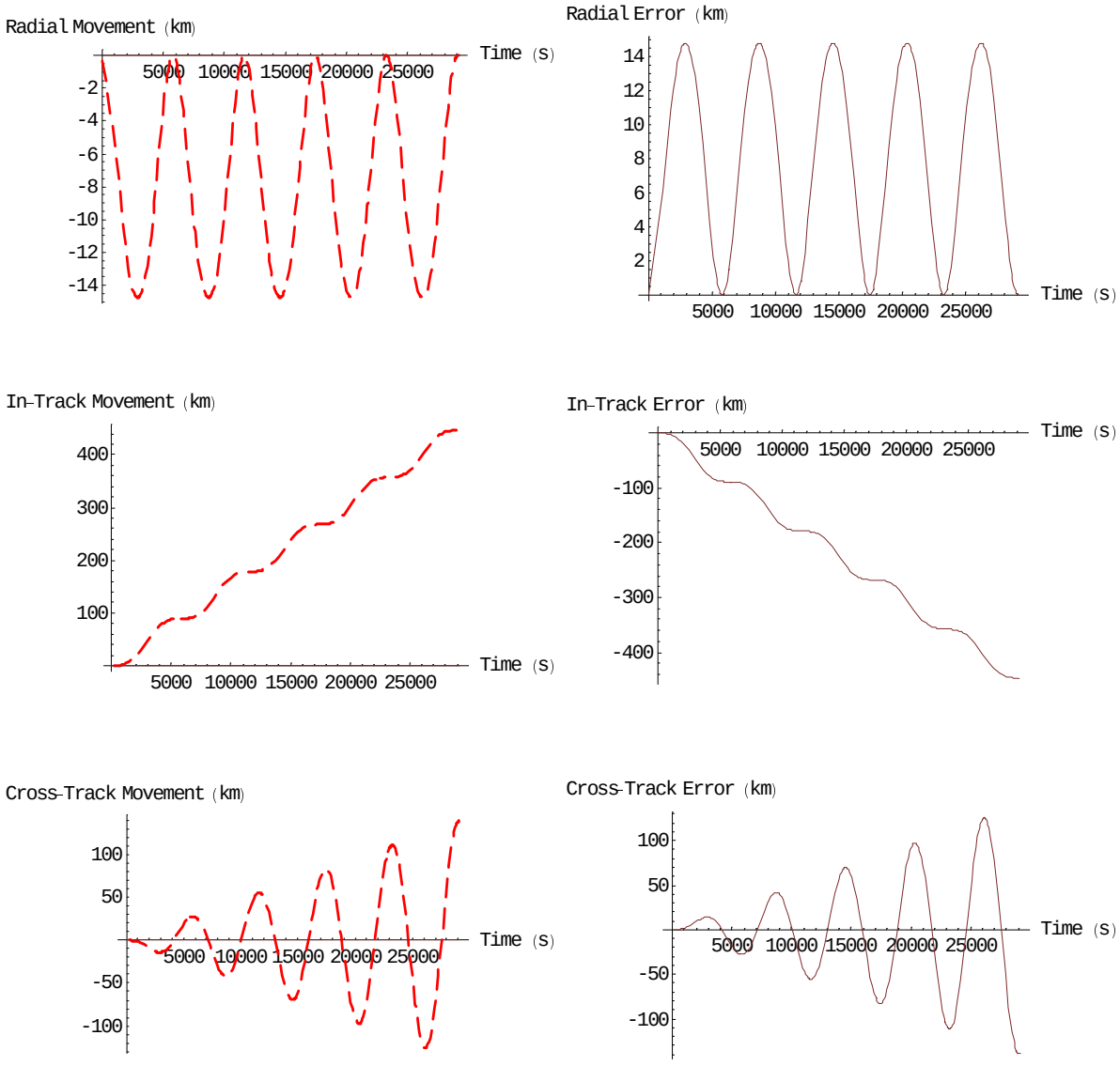

Figure 4-2 : Origin Motion – Hill's Equations

From Figure 4-2, it can be seen that Hill's equations do not capture the motion of the cluster's origin with respect to the reference orbit very well. According to Hill's equations, the cluster's origin should coincide exactly with the reference orbit. In the unperturbed case, this is true, but in the presence of the J_2 disturbance, Hill's equations fail.

In the radial direction, the origin of the cluster has periodic error of over 14 km. Under the influence of the J_2 disturbance, the cluster as a whole will "bob" up and down as the cluster passes over the areas of high and low mass concentrations respectively.

In the tangential direction, the reference orbit, and the cluster origin separate due to a difference in orbital periods. Under the J_2 disturbance, a satellite will have a different orbital period than it would in the unperturbed case. It was for this reason that the period of the reference orbit was sped up in the new linearized equations.

The error in the cross-track direction is due to the fact that the origin of the cluster has a drift in the longitude of the ascending node. Under the influence of the J_2 disturbance force, a satellite's longitude of the ascending node will precess. Hill's equations do not take this into account and thus there is a large increasing periodic error introduced.

4.3.2 The New Linearized Equations – Absolute Motion – Solution 1

In the first solution of the new linearized equations of motion, many changes were made to Hill's equations. The reference orbit is no longer a Keplerian reference orbit, but instead has a modified period. The J_2 disturbance force was introduced as a forcing function, and the gradient of the J_2 force was also incorporated into the equations of motion. These changes allow the new linearized equations to capture much of the motion due to the J_2 disturbance. The parameters of the reference orbit is

$$\begin{aligned} r_{ref} &= 7000 \text{ km} \\ i_{ref} &= 35^{\circ} \\ \omega_f &= n\,c \approx 0.00107837506 \text{ 1/sec} \end{aligned} \tag{4.19}$$

The location of the cluster origin is given with the following zero-drift parameters as calculated by the linearized equations.

$$\begin{aligned} x_0 &= 0 \quad \dot{x}_0 = \frac{n\, y_0}{2\, c}\left(2 - c^2\right) = 0 \\ y_0 &= 0 \quad \dot{y}_0 = -2n\, c\, x_0 + \frac{3n\, J_2\, R_e^2}{8\, c\, r_{ref}}(1 - Cos\, 2i_{ref}) \approx 0.00167306 \text{ km/s} \\ z_0 &= 0 \quad \dot{z}_0 = 0 \end{aligned} \tag{4.20}$$

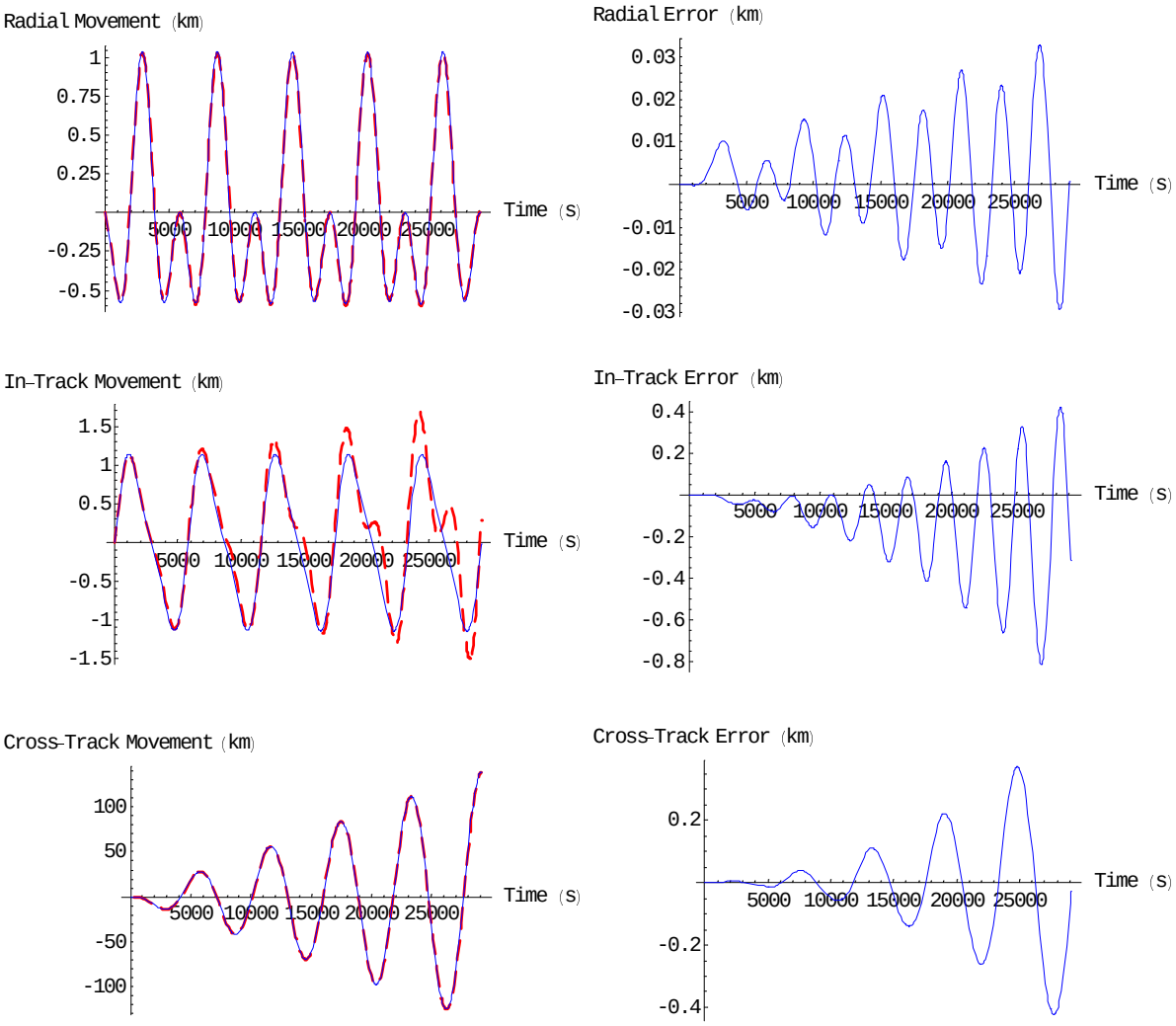

Figure 4-3 : Numerical Solution – Absolute Motion – Solution 1

From Figure 4-3 it can be seen that the errors from the initial linearized equations are much less than those created by Hill's equations. The 1st solution of the linearized equations produces an increasing periodic error of only 6 meters per orbit in the radial direction. This is much improved from the 14 km error in Hill's equations.

In the in-track direction, there is both a secular error and an increasing periodic error. The secular error is approximately 60 meters per orbit, and the increasing periodic error is 100 meters per orbit. This is also a large improvement over Hill's equations that have a secular error of 100 km/orbit. The increasing periodic error is due to the fact that the orbital planes are separating, and the in-track motion is changing shape as a result.

Finally the cross-track direction has an increasing periodic error of approximately 100 meters per orbit. Again this is an improvement over Hill's equations that had an error of 30 km per orbit.

4.3.3 The New Linearized Equations – Absolute Motion – Solution 2

In the 2nd solution of the linearized equations of motion, the reference orbit was changed so that it had the same variation in the longitude of the ascending node as the cluster origin. This was accomplished by incorporating the normal component of the J_2 disturbance force into the reference orbit.

From equation (3.29), the equation of motion of the reference orbit is given as

$$\begin{aligned}\vec{r}_{ref} &= r_{ref}(Cos\,\Omega\,Cos\,\theta - Sin\,\Omega\,Sin\,\theta\,Cos\,i)\hat{X} \\ &+ r_{ref}(Sin\,\Omega\,Cos\,\theta + Cos\,\Omega\,Sin\,\theta\,Cos\,i)\hat{Y} \\ &+ r_{ref}(Sin\,\theta\,Sin\,i)\hat{Z}\end{aligned} \tag{4.21}$$

with

$$
\begin{aligned}
i(t) &\approx i_0 - \frac{3\sqrt{\mu} J_2 R_e^2}{2 k r_{ref}^{7/2}} Cos\, i_{ref}\ Sin\, i_{ref} \\
\Omega(t) &\approx \Omega_0 - \frac{3\sqrt{\mu} J_2 R_e^2}{2 r_{ref}^{7/2}} t\, Cos\, i_{ref} \\
\theta(t) &\approx k\, t
\end{aligned}
\tag{4.22}
$$

The reference orbit parameters are

$$
\begin{aligned}
r_{ref} &= 7000 \text{ km} \\
i_{ref} &= 35^{\circ} \\
\omega_f &= n\, c = 0.00107837506 \text{ 1/sec}
\end{aligned}
\tag{4.23}
$$

The origin of the reference orbit is given with the following zero-drift parameters as calculated by the new linearized equations.

$$
\begin{aligned}
&x_0 = 0 \quad \dot{x}_0 = \frac{n\, y_0}{2\, c}\left(2 - c^2\right) = 0 \\
&y_0 = 0 \quad \dot{y}_0 = -2 n\, c\, x_0 + \frac{3 n^2\, J_2\, R_e^2}{8 k\, r_{ref}}(1 - Cos\, 2 i_{ref}) \approx 0.00167155 \text{ km/s} \\
&z_0 = 0 \quad \dot{z}_0 = 0
\end{aligned}
\tag{4.24}
$$

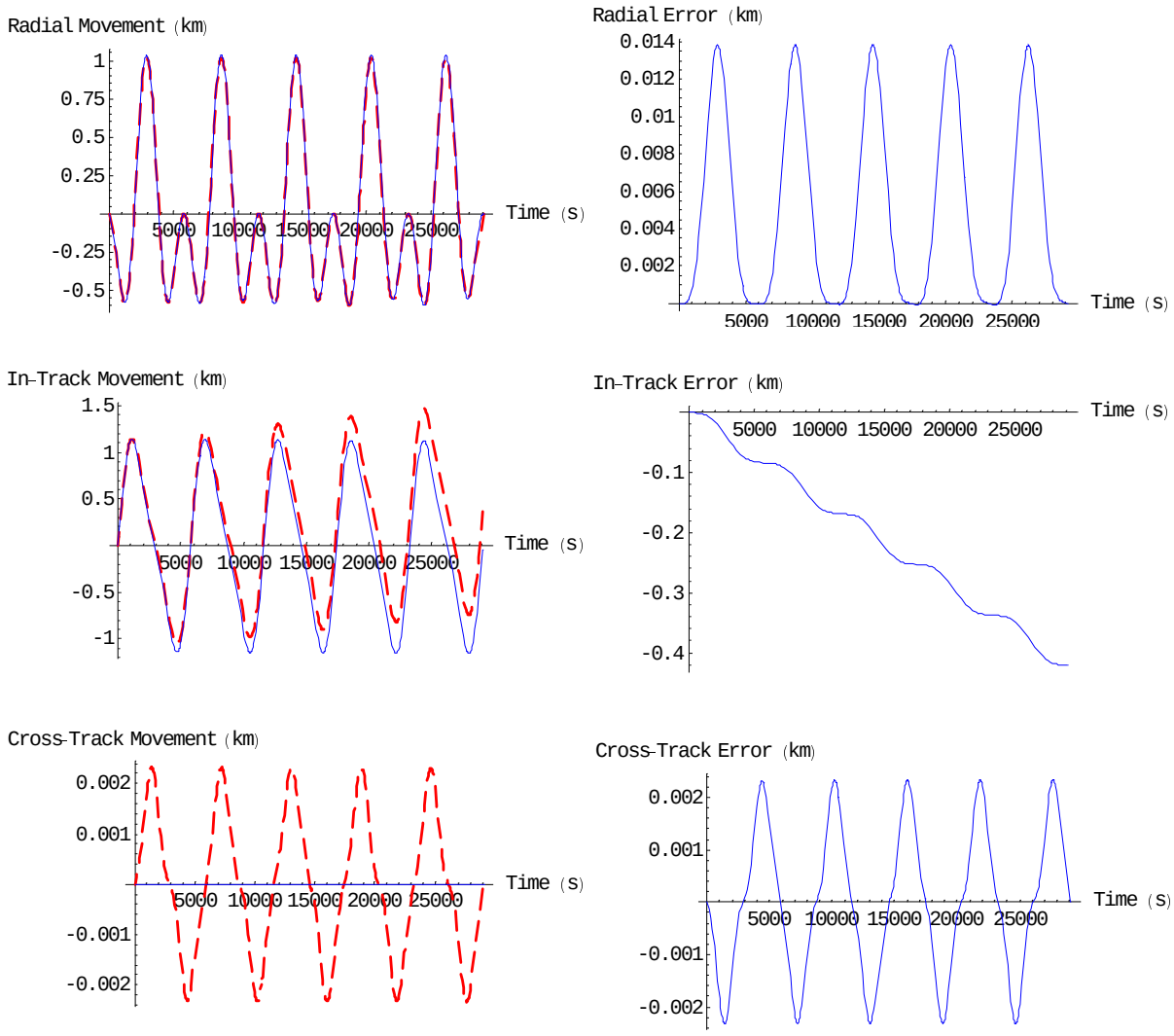

Figure 4-4 : Numerical Solution – Absolute Motion – Solution 2

By changing the reference orbit, the radial error has now been reduced to a constant periodic error of only 14 meters. This is an improvement of three orders of magnitude when compared to Hill's equations.

In the in-track direction, there is still a secular drift of 100 meters per orbit, but the increasing periodic error has now been removed since the satellite remains close to the reference orbit.

Finally, since the reference orbit's longitude of the ascending node is moving at the same rate as the perturbed satellite, there is no cross-track error except for a small periodic error of 2 meters. This error is due to the fact that the reference orbit is not completely modeled correctly and some errors were introduced as a result.

4.3.4 Conclusions – Absolute Motion

Figure 4-5 combines all the errors shown above and allows for comparison between Hill's equations, and the two solutions. The plots on the left side are plots of the errors. The plots on the right are plots of the same errors, just zoomed in to allow the differences between the 1^{st} and 2^{nd} solution to be seen more easily.

From Figure 4-5, it can be seen that Hill's equations do not capture the absolute motion of the cluster under the influence of the J_2 disturbance force. The errors are large, on the order of kilometers.

The first solution shows a marked improvement in the motion of these terms. Errors were reduced from kilometers to meters. The second solution showed even more improvements by eliminating increasing periodic terms.

Currently the average J_2 disturbance force is calculated by using the reference orbit. This is done because the reference orbit has a constant radius and constant angular rate. However, this is not same as the average J_2 force affecting the perturbed satellite. The result is an error in the new analytically determined orbital period of the reference orbit, and a drift in the in-track direction. This error can be corrected numerically, and a relationship that would zero this drift can be created that is a function of inclination. However, this correction factor is not determined in this thesis.

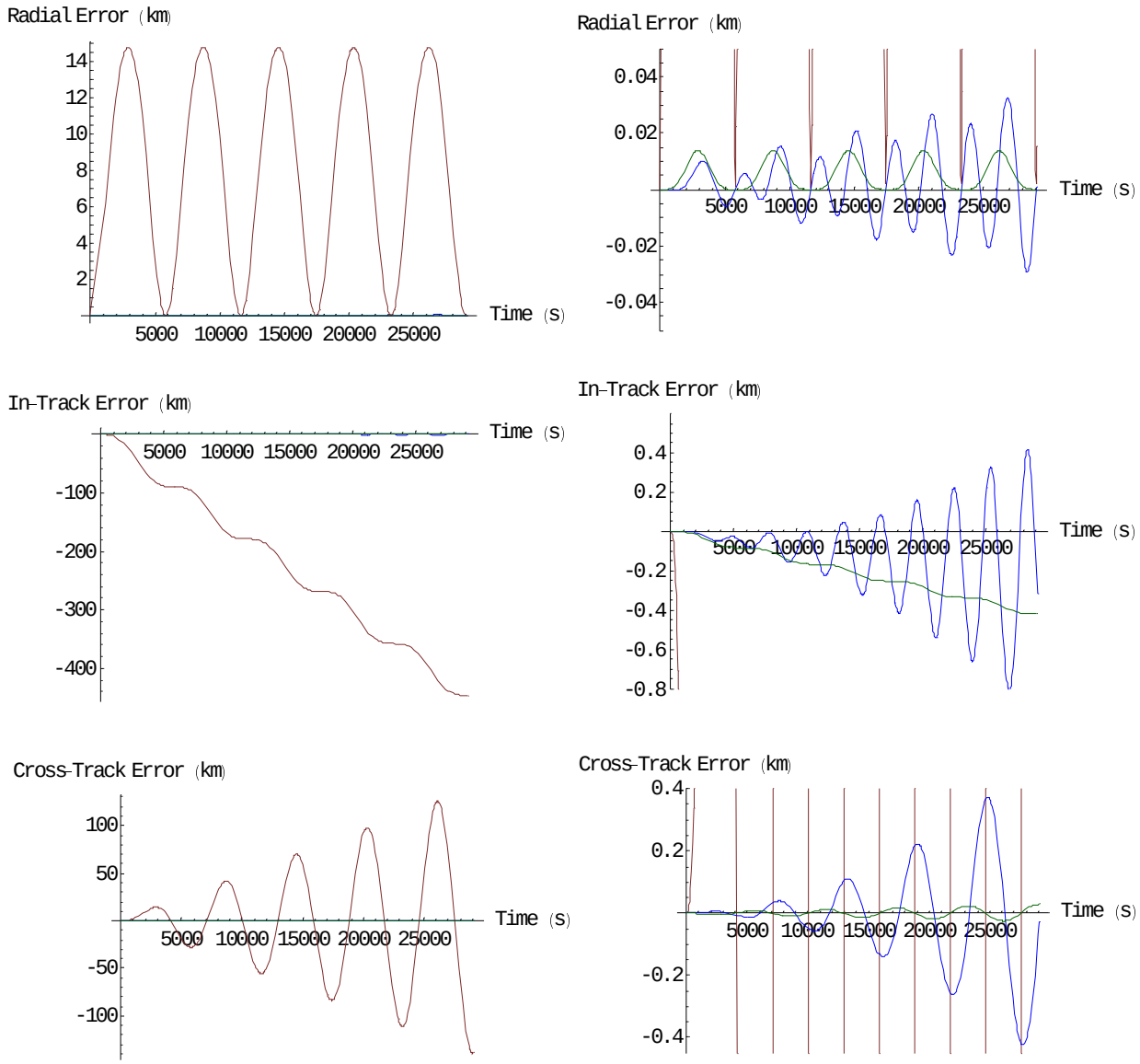

Figure 4-5 : Absolute Movement Errors – Combined Plots

4.4 Relative Motion

While the absolute motion with respect to the reference orbit is important for some applications, the relative motion of satellites within the cluster is equally important. In this next section, the relative motion of a satellite with respect to the cluster origin or alternatively a second satellite will be calculated and compared to a numerical simulation. Once again, Hill's equations will be used as a benchmark to compare the performance of the new linearized equations of motion.

In order to better characterize the errors, each initial condition will be varied independently. There are six different initial conditions that can be specified. Three position components (x_o, y_o, z_o), and three velocity components $(\dot{x}_o, \dot{y}_o, \dot{z}_o)$. However, for zero-offset, and zero-drift conditions, two of the initial velocity components can again be solved for. These initial velocities vary depending on the specific linearized equations used.

The initial conditions will be such that each satellite will be a maximum of 100 meters away from the origin of the cluster. The initial conditions for the origin of the cluster will be those calculated with the 2nd solution.

4.4.1 Radial Offset

The first parameter to be varied will be an offset in the radial direction. The satellite will start off 100 meters away in the radial direction from the cluster origin.

4.4.1.1 Hill's Equations

Once again, Hill's equations are used as a benchmark. The initial conditions for the satellite are

$$\begin{aligned} x_0 &= 0.1\,\text{km} & \dot{x}_0 &= \frac{n\,y_0}{2} = 0 \\ y_0 &= 0 & \dot{y}_0 &= -2\,n\,x_0 = \text{-0.000215601403 km/s} \\ z_0 &= 0 & \dot{z}_0 &= 0 \end{aligned} \tag{4.25}$$

These initial conditions result in the following plots.

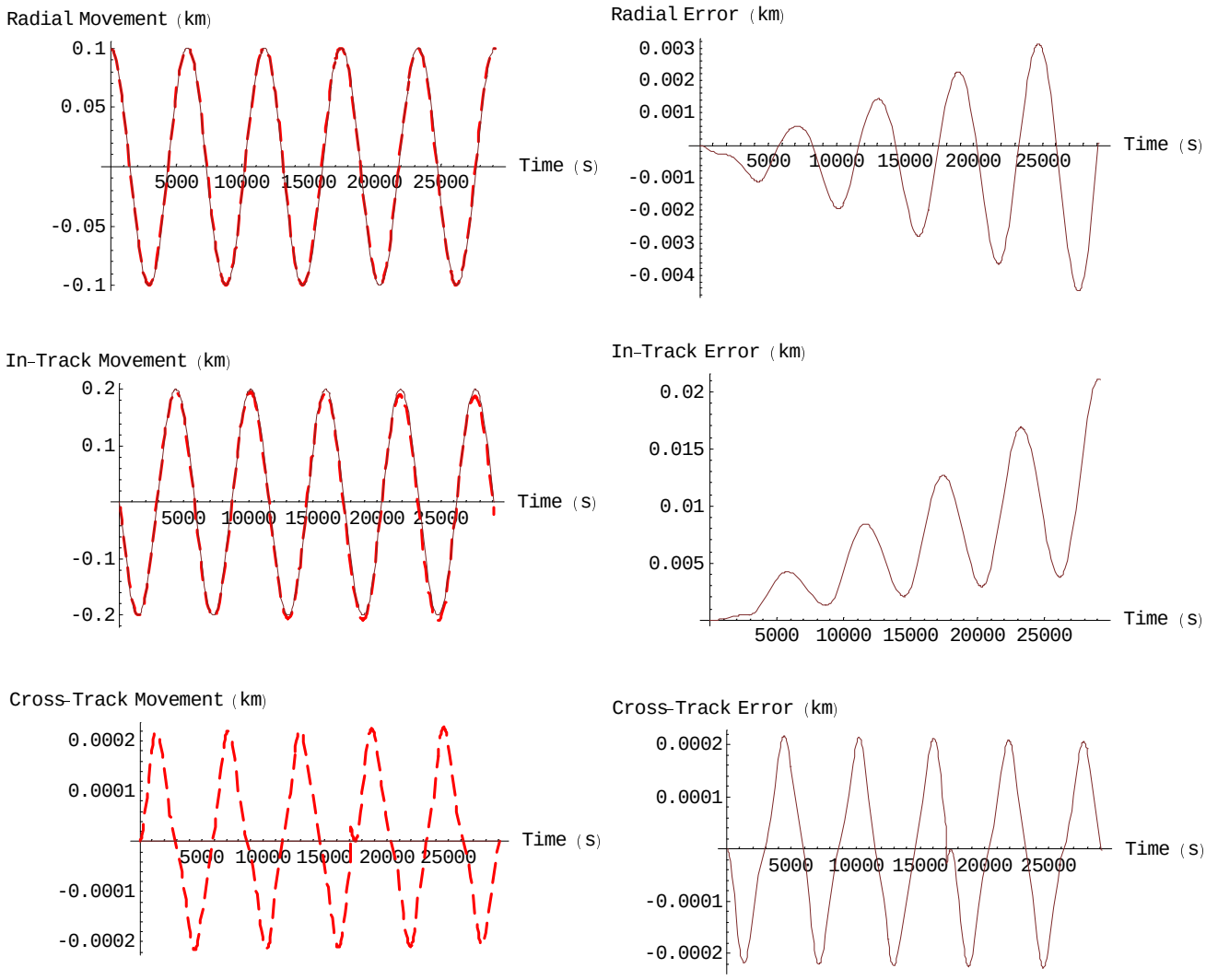

Figure 4-6 : Hill's Equations – Relative Motion – Radial Offset

The plots on the left side of the page are the actual and calculated movements of the satellite in the radial, in-track, and cross-track direction with the errors on the right.

In the radial direction, there is an increasing periodic error. This periodic error increases in amplitude at about 1 meter per orbit. The error in the radial direction is caused by the incorrect period of the periodic terms in the radial direction. Over time, the two periodic

motions, (numerical and Hill's), become more and more out of phase, and the error grows.

In the in-track direction there is both a secular error, and a periodic error. The secular error increases at a rate of about two meters per orbit. The secular error is caused by a mismatch in the period of the satellite and the origin of the cluster. Essentially, Hill's equations gives initial conditions that are not truly closed orbits, and the satellite is placed into an orbit that does not have the same period as the cluster origin.

The periodic error in the in-track direction increases at a rate of about one meter per orbit. The reason for this error is similar to that of the error in the radial direction. Hill's equations specify the wrong period for the periodic terms in the in-track direction.

Finally, there is a small periodic error in the cross-track direction of approx 20 cm. The amplitude of this error does not increase. This error is due to the fact that Hill's equations assume that the earth is perfectly spherical. However, the effect of the J_2 disturbance does cause periodic movement in the cross-track direction that is not captured.

4.4.1.2 Relative motion

The new linearized equations of motion will be used. The initial position conditions will remain the same, but some of the initial velocities will change. These velocities are chosen to represent the zero-drift/zero-offset conditions given by the new equations themselves. The first set of parameters is given as

$$\begin{aligned} x_0 &= 0.1\,\text{km} \quad & \dot{x}_0 &= \frac{n\,y_0}{2\,c}\left(2-c^2\right)=0 \\ y_0 &= 0 & \dot{y}_0 &= -2n\,c\,x_0 \approx \text{-0.000215675 km/s} \\ z_0 &= 0 & \dot{z}_0 &= 0 \end{aligned} \tag{4.26}$$

The results of the simulation are shown in Figure 4-7.

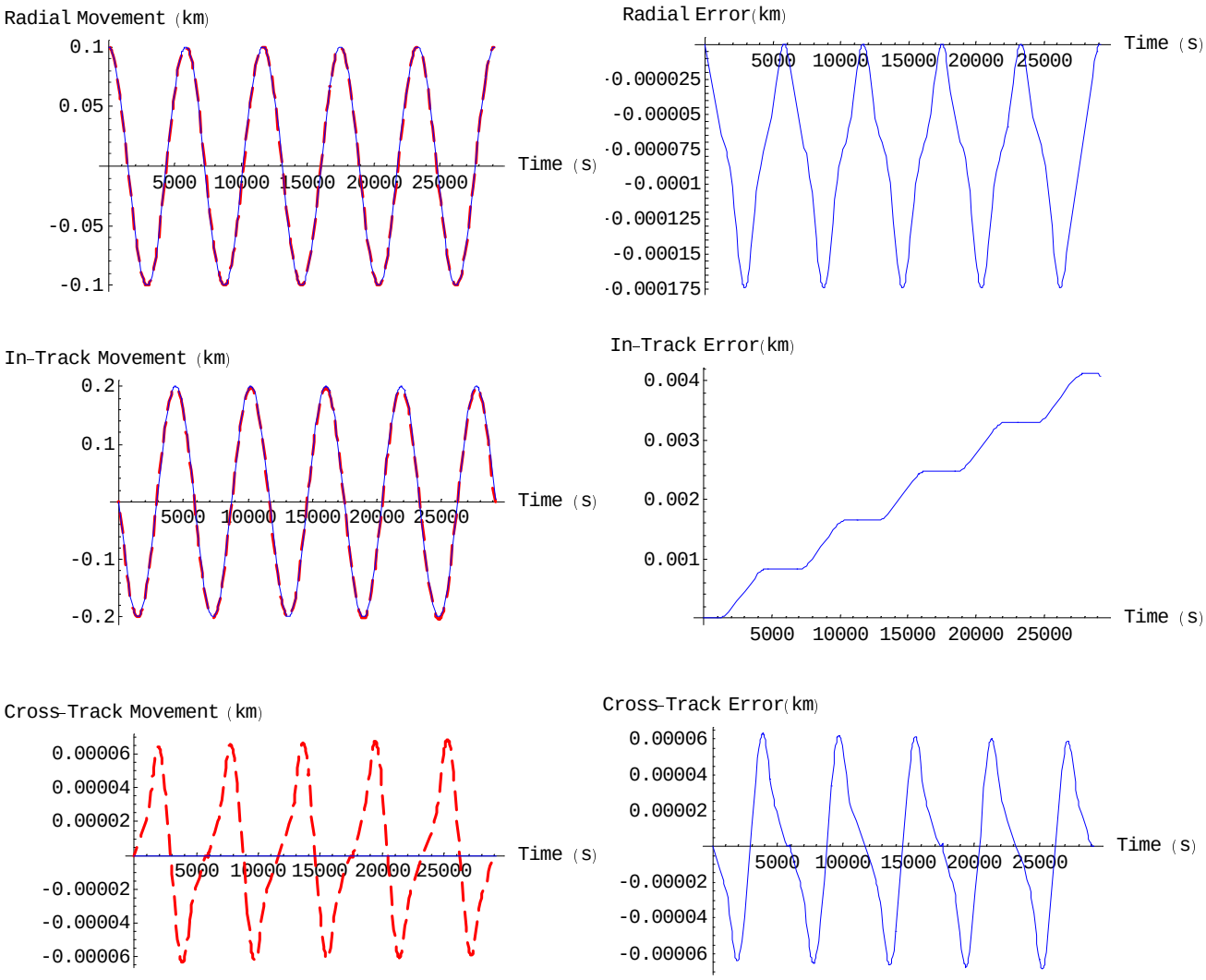

Figure 4-7 : New Linearized Equations – Relative Motion – Radial Offset

In the radial direction, the increasing periodic error that was present in Hill's equations has been eliminated. Now the only error is a periodic error of 17 cm. This small error is due to the fact that a time averaged J_2 disturbance is used to calculate the gradient of the J_2 disturbance force, and thus small periodic variations are not captured.

In the in-track direction, the increasing periodic error has also been eliminated. There is, however, still a secular drift. This drift is on the order of 1 m per orbit, and is again due to an orbital period mismatch due to incorrect initial velocity conditions.

The error in the cross-track direction did not change very much, but has been reduced to a periodic error of only 6 cm.

4.4.1.3 Relative motion with corrected initial conditions

In this version of the linearized equations of motion, the error in the initial conditions due to the linearization of the gravity terms is removed. While the initial conditions used are not the exact initial conditions specified by the new linearized equations of motion, they are the initial conditions that match the orbital period of the satellite to that of the reference orbit.

The new initial conditions are

$$\begin{aligned} x_0 &= 0.1\text{km} & \dot{x}_0 &= \frac{n\,y_0}{2\,c}\left(2-c^2\right)=0 \\ y_0 &= 0 & \dot{y}_0 &\approx \text{-0.000215722 km/s} \\ z_0 &= 0 & \dot{z}_0 &= 0 \end{aligned} \tag{4.27}$$

It should be noted that the change in the initial velocity is only $47\ \mu$m/s. This shows the strong sensitivity of the in-track motion to the velocity. The plots are shown below.

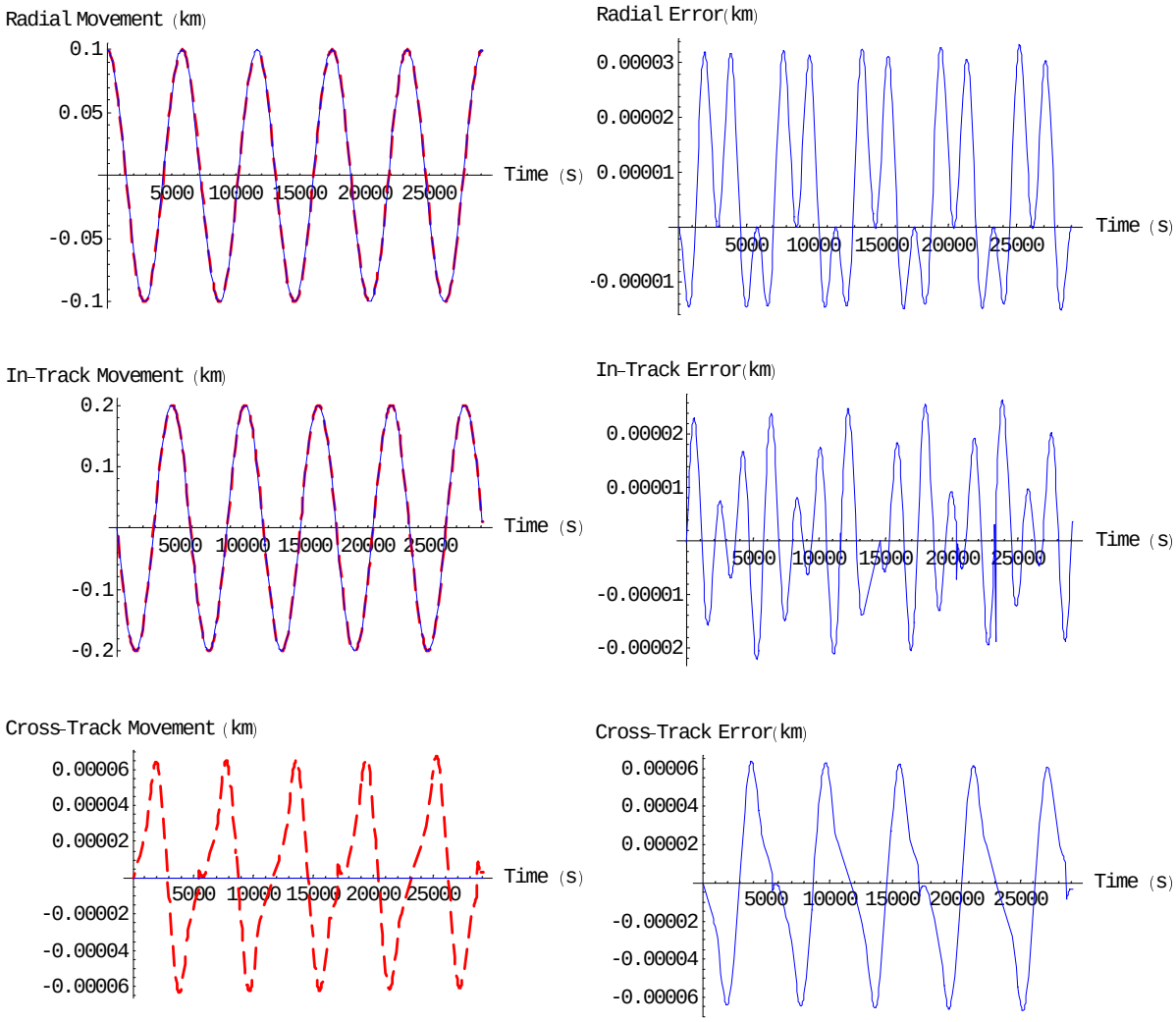

Figure 4-8 : New Linearized Equations – Relative Motion – Radial Offset

The error in the radial direction has now improved to become a periodic error of only 3 cm. In the in-track direction, the error no longer has a secular component, but instead is periodic with a magnitude of only a little more than 2 cm. The cross-track error remains unchanged with a periodic error of 6 cm.

It should be noted that this version of the equation produces no errors that increase appreciably over time.

4.4.2 In-Track Offset

The next simulation will be an offset in the in-track direction of 100 meters. Normally, an offset in the in-track direction will remain as a constant offset in the in-track direction. However, the initial velocity conditions were selected such that there is no offset, and thus the satellite is placed into a free orbit ellipse around the origin of the cluster.

$$\begin{aligned} x_0 &= 0 & \dot{x}_0 &= \frac{n\,y_0}{2} \approx 0.0000539004 \text{ km/s} \\ y_0 &= 0.1 \text{ km} & \dot{y}_0 &= -2\,n\,x_0 = 0 \\ z_0 &= 0 & \dot{z}_0 &= 0 \end{aligned} \tag{4.28}$$

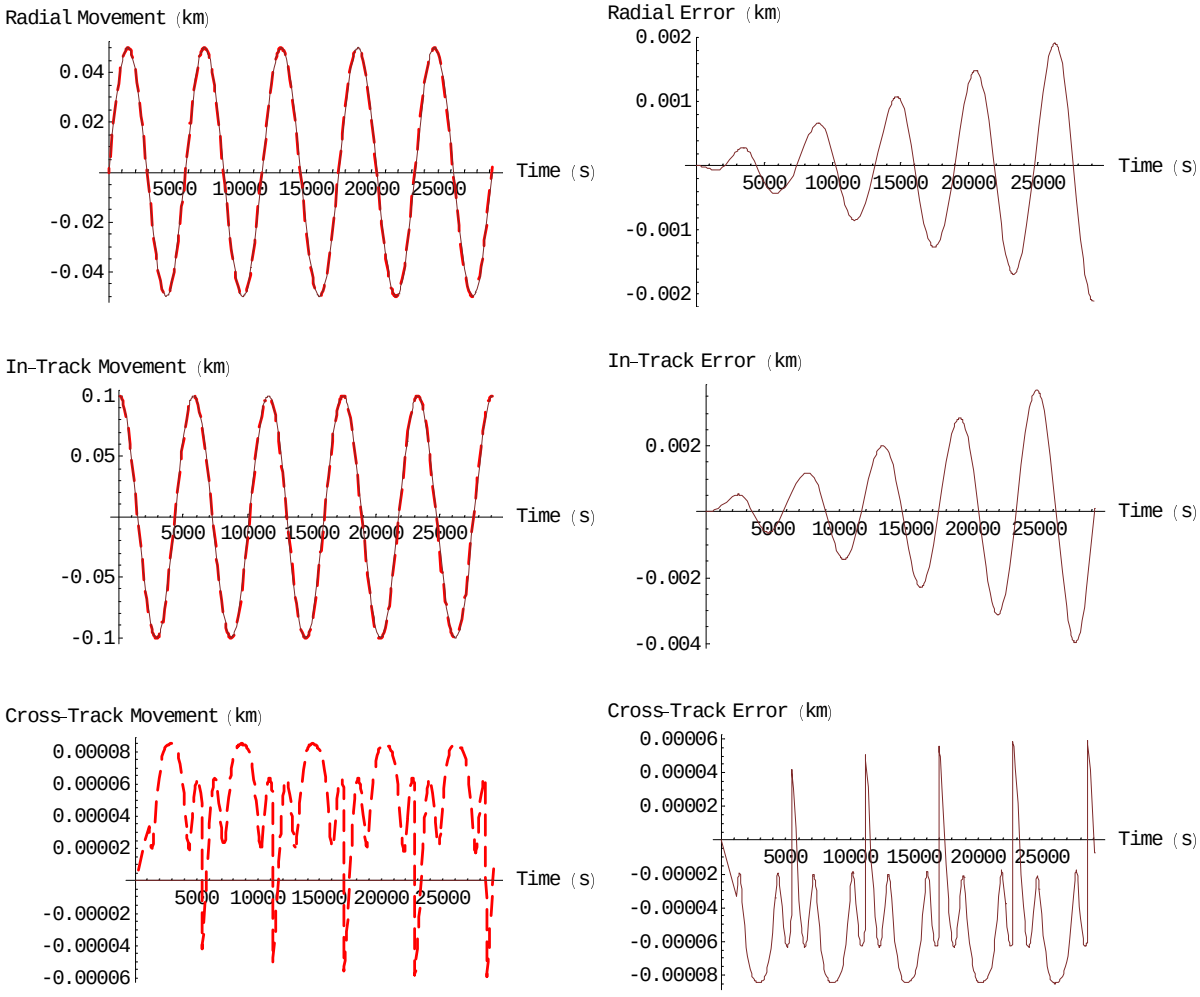

Figure 4-9 : Hill's Equations – Relative Motion – In-Track Offset

In this case, both the radial and the in-track direction experience an increasing periodic error of approximately 0.5 m per orbit. This error is once again due to a mis-match in the period of the periodic x and y terms. The cross-track error is also once again periodic with a magnitude of 8 cm, but is not increasing in time.

4.4.2.1 Relative Motion

Once again, the initial conditions for the new linearized equations of motion are calculated. The parameters for the in-track offset are

$$\begin{aligned} x_0 &= 0 & \dot{x}_0 &= \frac{n\,y_0}{2\,c}\left(2-c^2\right) = 0.0000538452 \text{ km/s} \\ y_0 &= 0.1\text{km} & \dot{y}_0 &= -2n\,c\,x_0 = 0 \\ z_0 &= 0 & \dot{z}_0 &= 0 \end{aligned} \tag{4.29}$$

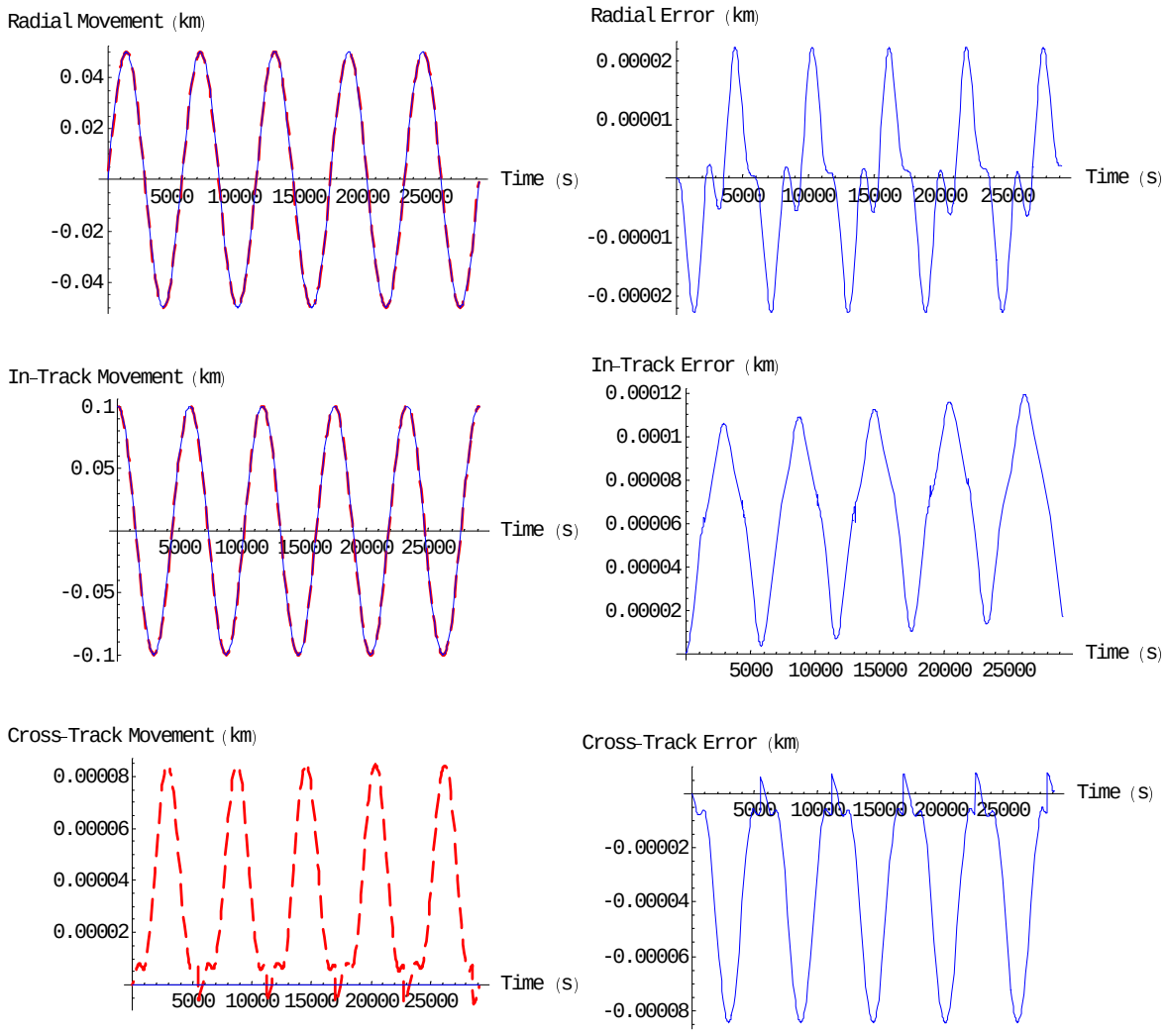

Figure 4-10 : New Linearized Equations – Relative Motion – In-Track Offset

The radial direction has a periodic error of 2 cm. The in-track error is also periodic with an error of 11 cm. There is also a small secular error present in the in-track direction with a magnitude of 0.2 cm/orbit. The cross-track direction has a periodic error of less than 9 cm. These are once again a marked improvement over Hill's equations.

4.4.2.2 Relative motion with corrected initial conditions

Because there is only an offset in the y-direction, the error in the initial conditions is very small. This resulted in a small secular drift in the y-direction of only 0.2 cm per orbit. However, this can still be removed. The new initial conditions are…

$$\begin{aligned} x_0 &= 0 & \dot{x}_0 &= \frac{n\,y_0}{2\,c}\left(2-c^2\right) = 0.0000538452 \text{ km/s} \\ y_0 &= 0.1\text{km} & \dot{y}_0 &\approx 0 \\ z_0 &= 0 & \dot{z}_0 &= 0 \end{aligned} \tag{4.30}$$

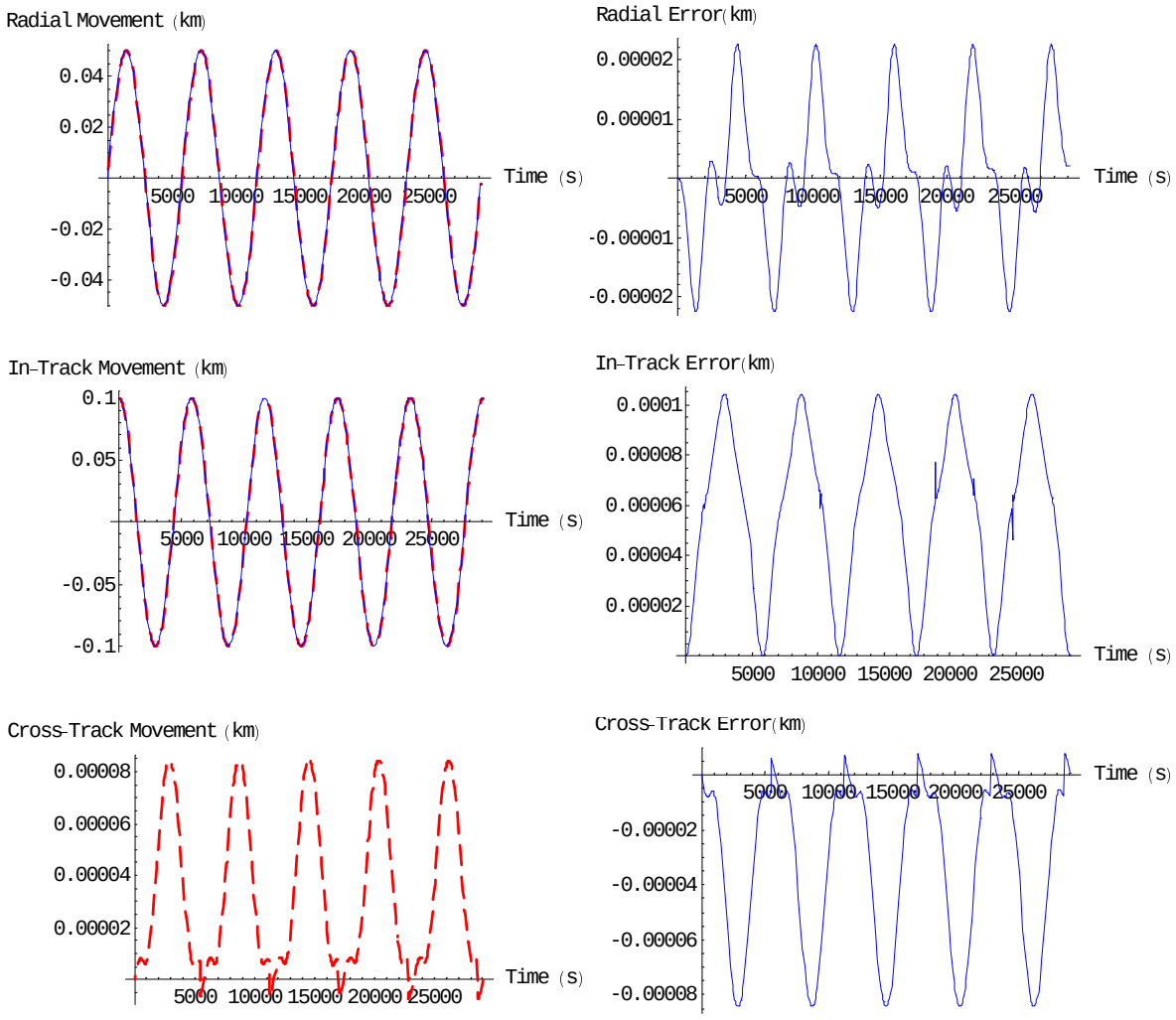

Figure 4-11: New Linearized Equations – Relative Motion – In-Track Offset

From Figure 4-11, it can be seen that the secular drift in the in-track direction has once again been removed. The motion in the other two directions remains unchanged.

4.4.3 Cross-Track Offset

The previous two simulations were variations that kept the satellite in the same plane of motion as the center of the cluster. The next two sections will generate out of plane motion.

4.4.3.1 Hill's Equations

The next simulation is an offset in the cross-track direction with the following parameters

$$\begin{aligned} x_0 &= 0 & \dot{x}_0 &= \frac{n\, y_0}{2} = 0 \\ y_0 &= 0 & \dot{y}_0 &= -2\, n\, x_0 = 0 \\ z_0 &= 0.1 \text{ km} & \dot{z}_0 &= 0 \end{aligned} \tag{4.31}$$

Looking at Figure 4-12, there is no offset in the $\hat{x}$ or $\hat{y}$ direction, and Hill's equations state that there is no movement in the $\hat{x}$ or $\hat{y}$ direction. As a result, there is no period mismatch, and thus no increasing periodic error. There is still a small periodic error on the order of 5 cm in the radial direction, and 20 cm in the tangential direction.

In the cross-track direction there is an increasing periodic error. Because both the satellite and the origin of the cluster have very similar inclinations, there is no differential drift in the longitude of the ascending node. The increasing periodic error is due to a difference in the period of the $\hat{z}$ terms. The error is increasing at a rate of approximately 1.5 meter per orbit.

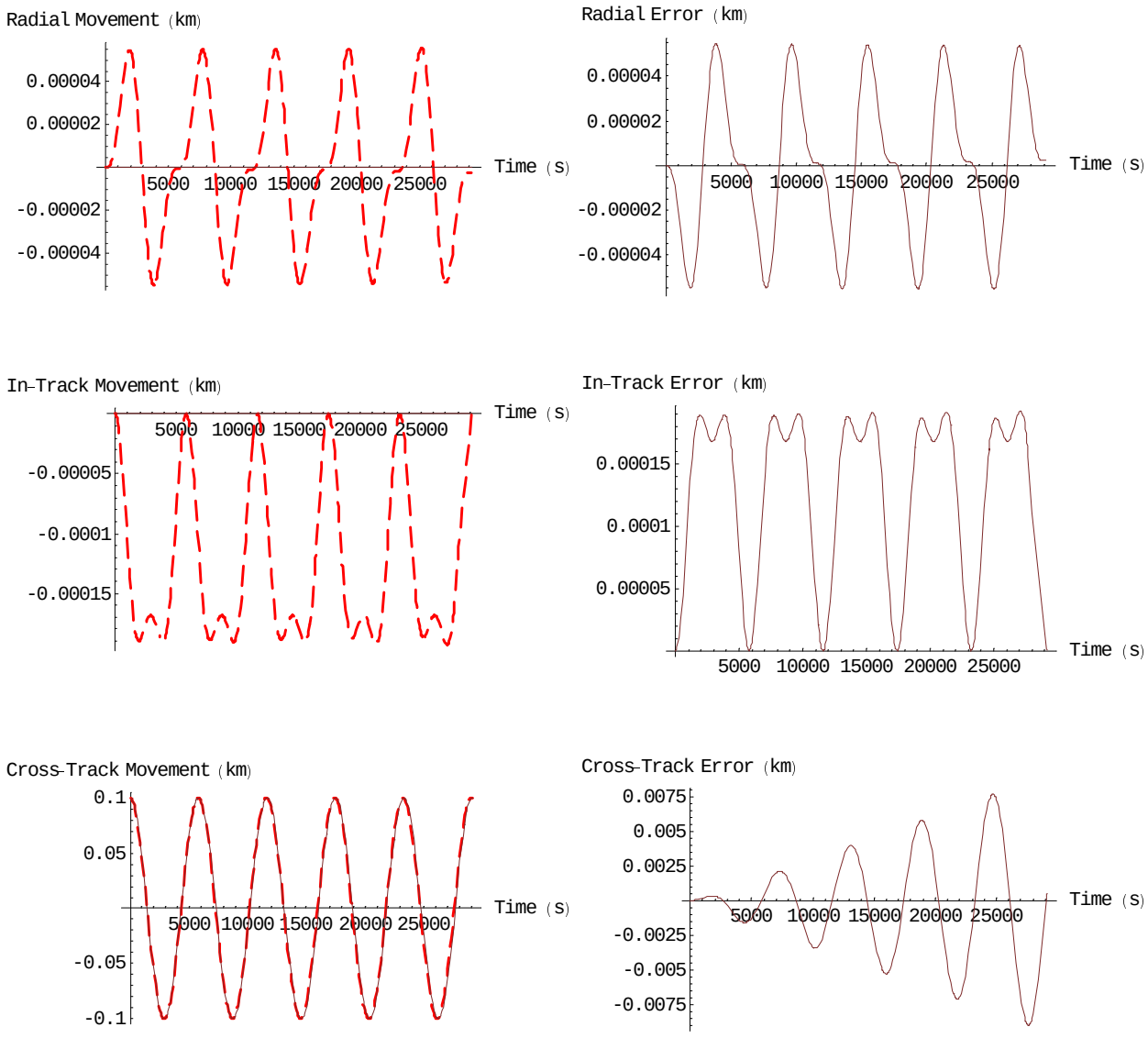

Figure 4-12: Hill's Equation – Relative Motion – Cross-Track Offset

4.4.3.2 Relative motion

The parameters for the cross-track direction are

$$\begin{aligned} x_0 &= 0 & \dot{x}_0 &= \frac{n\,y_0}{2\,c}\left(2-c^2\right)=0 \\ y_0 &= 0 & \dot{y}_0 &= -2nc\,x_0 = 0 \\ z_0 &= 0.1\text{km} & \dot{z}_0 &= 0 \end{aligned} \tag{4.32}$$

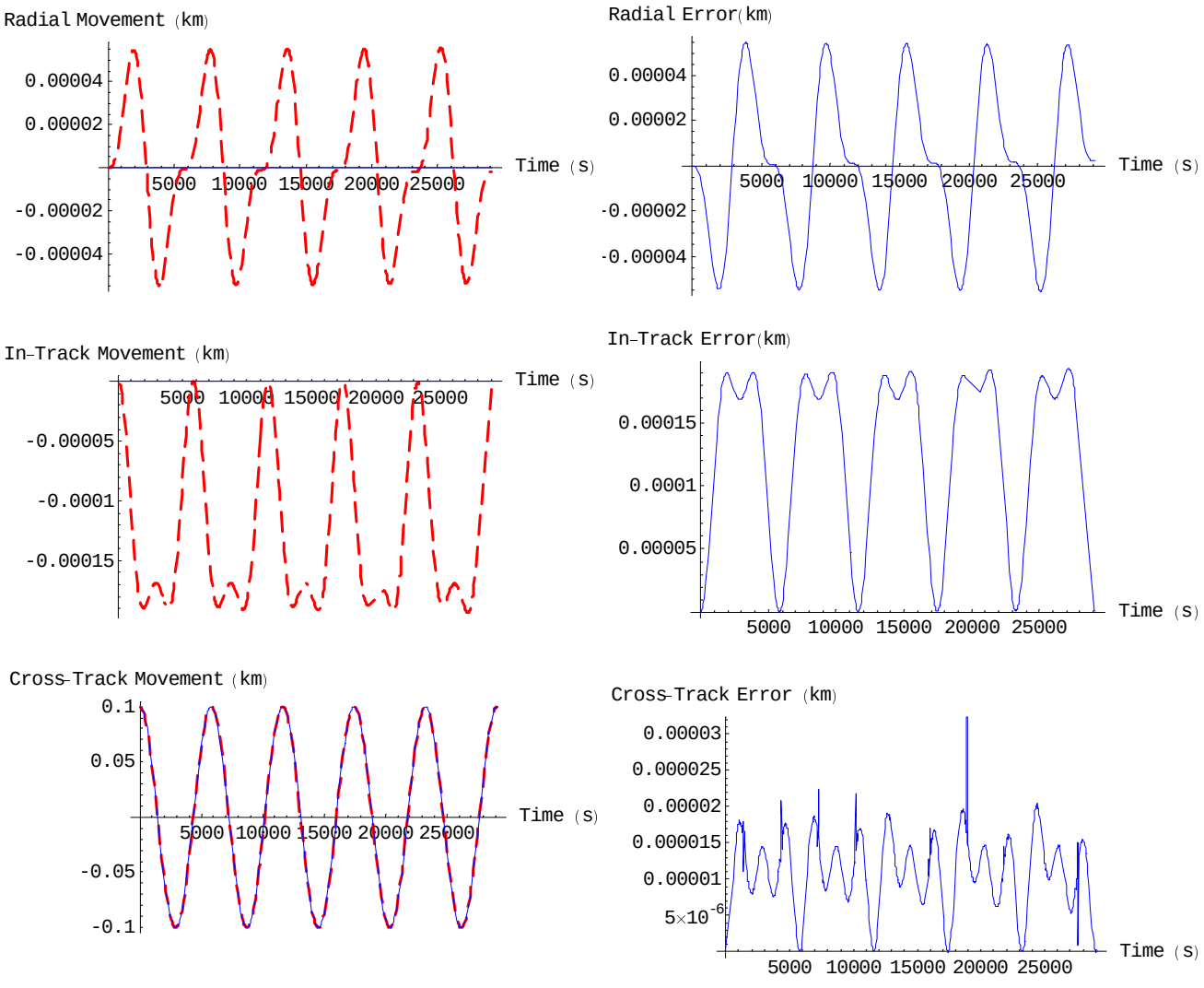

Figure 4-13: New Linearized Equations – Relative Motion – Cross-track Offset

The new linearized equations offer the same amount of error in the radial and in-track direction, 6 cm and 20 cm respectively. However, the cross-track motion has been captured by the equations, resulting in a periodic error of less than 2 cm.

4.4.3.3 Relative Motion with Corrected Initial Conditions

Because the satellite started with the same radius and inclination as the reference satellite, there is no error in the initial conditions. Because there is no change, the results are not shown here.

4.4.4 Cross-Track Velocity Offset

The final simulation is slightly different than the previous three. In each of those, the position of the satellite was varied, and the initial velocity conditions were calculated for zero drift conditions. In this case, the fourth initial condition to vary is a velocity. Both the satellite and the center of the cluster start in the same location, but the satellite has an initial cross-track velocity. This causes an out of plane motion and places the satellite in a different inclination than the reference orbit

4.4.4.1 Hill's Equations

The initial parameters are

$$\begin{aligned} x_0 &= 0 \quad \dot{x}_0 = \frac{n\,y_0}{2} = 0 \\ y_0 &= 0 \quad \dot{y}_0 = -2\,n\,x_0 = 0 \\ z_0 &= 0 \quad \dot{z}_0 = 0.1n \approx 0.000107801 \text{ km/s} \end{aligned} \tag{4.33}$$

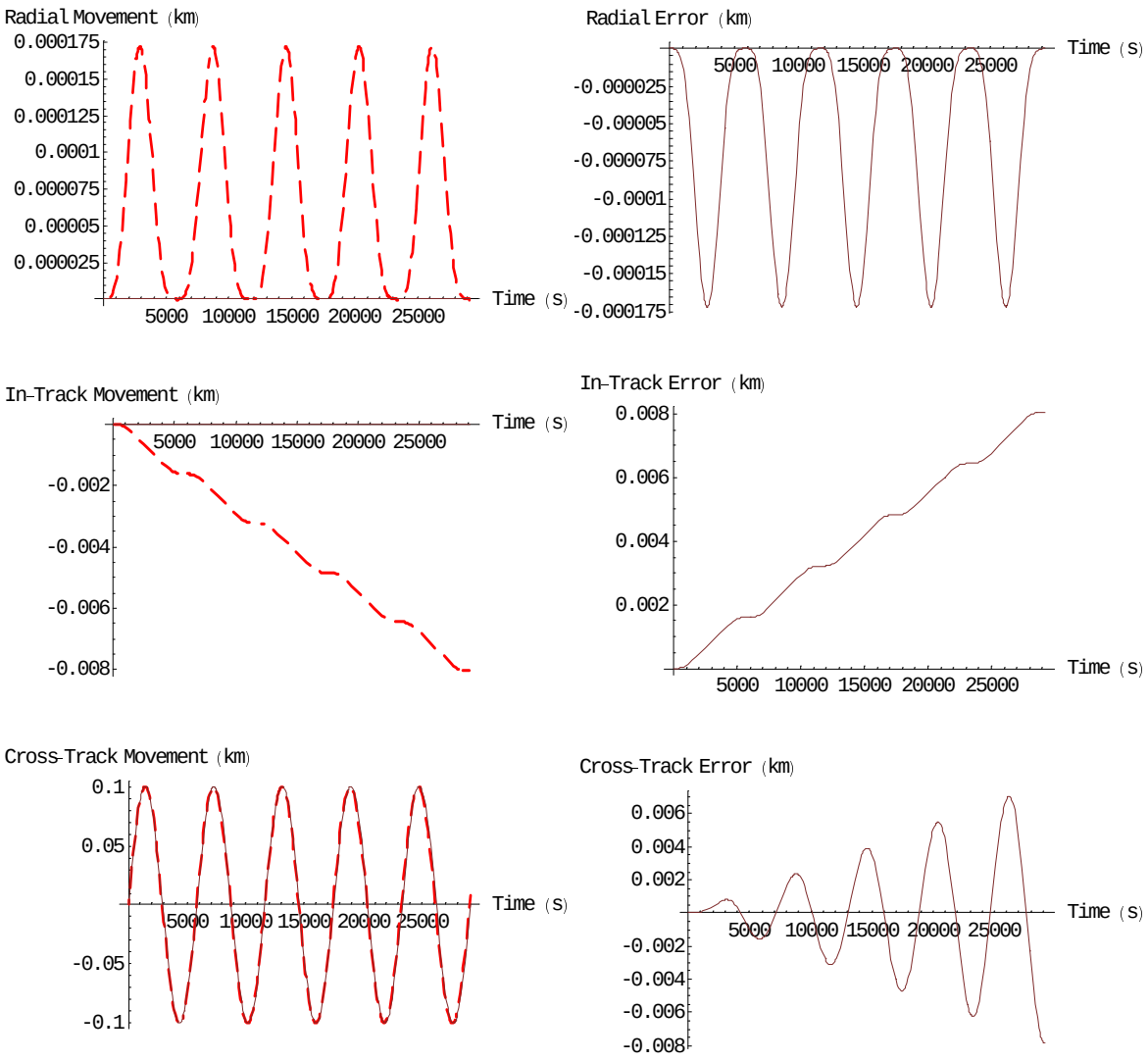

Figure 4-14: Hill's Equations – Relative Motion – Cross-Track Velocity Offset

Once again, Hill's equations state that there is no movement in the radial and in-track direction. There is still a small periodic error of 17mm in the radial direction. In the in-track direction, there is a secular error of approximately 0.9 m per orbit once again due to an orbital period mismatch. There is a cross-track error due to a period mismatch in the cross-track terms.

4.4.4.2 Relative motion

The initial parameters for the new linearized equations are

$$\begin{aligned} x_0 &= 0 \quad \dot{x}_0 = \frac{n\,y_0}{2\,c}\left(2-c^2\right)=0 \\ y_0 &= 0 \quad \dot{y}_0 = -2n\,c\,x_0 = 0 \\ z_0 &= 0 \quad \dot{z}_0 = 0.107911\text{m/s} \end{aligned} \tag{4.34}$$

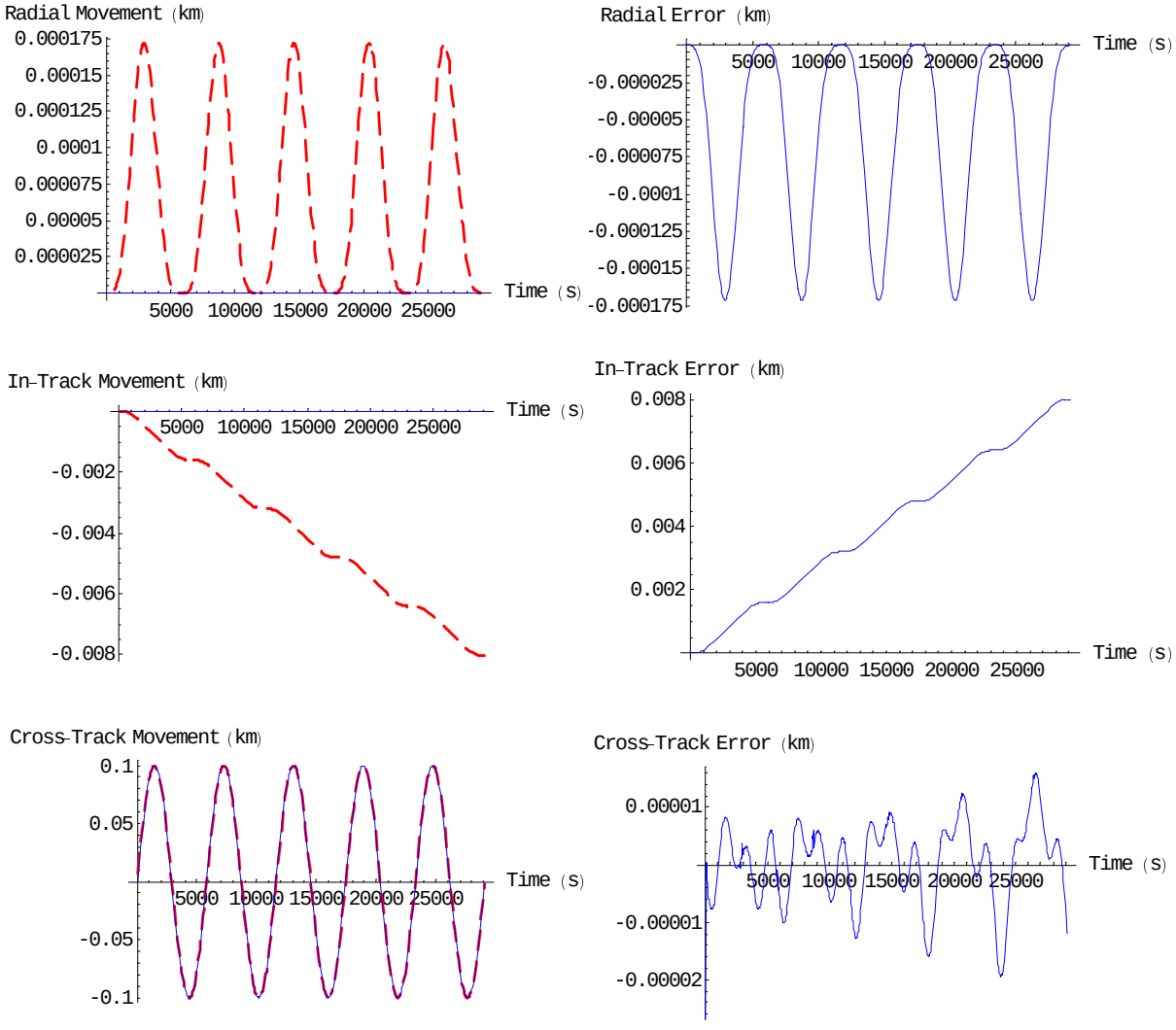

Figure 4-15: Linearized Equations – Relative motion – Cross-Track Velocity Offset

There is a slight periodic error in the radial direction of 16 cm. There is also a secular drift in the in-track direction once again to a period mismatch. The cross-track error has once again been captured with an error of 2 cm, but there appears to be a sight increase in the error over time. This has been attributed to a slight numerical error in calculating the effective inclination of the perturbed satellite.

4.4.4.3 Relative motion with new initial conditions

In the previous numerical simulations, all satellite orbital inclinations have been the same, or very nearly the same. In this simulation, the inclinations are not the same. There is a difference of 0.000819°. However this variation does cause the satellite to see a different average J_2 causing an orbital period mismatch. The correct initial velocities were found numerically. The initial conditions used are

$$\begin{aligned} x_0 &= 0 \quad \dot{x}_0 = \frac{n\, y_0}{2\, c}\left(2 - c^2\right) = 0 \\ y_0 &= 0 \quad \dot{y}_0 \approx 0.00000123505 \text{ km/s} \\ z_0 &= 0 \quad \dot{z}_0 = 0.000107911 \text{ km/s} \end{aligned} \tag{4.35}$$

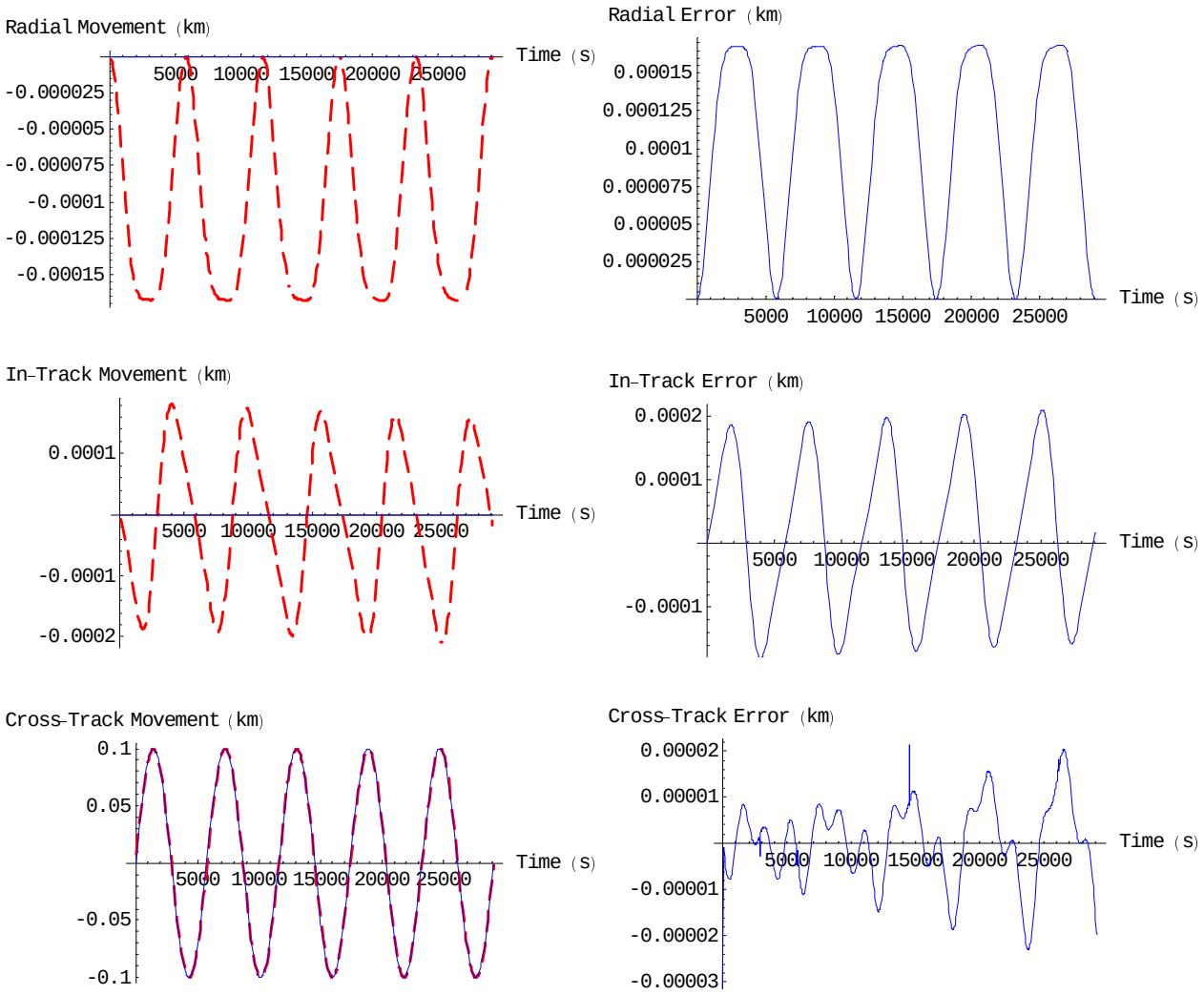

Figure 4-16 : Linearized Equations – Relative Motion – Cross Track Velocity Offset

Once again, by using the corrected initial conditions, the drift in the in-track direction have been reduced to a periodic error of only two cm.

4.5 Numerical Simulations Conclusions

4.5.1.1 Hill's Equations

Throughout this chapter, Hill's equations were used as a benchmark against which the new linearized equations were compared. When looking at the cluster motion as a whole, Hill's equations failed to capture the motion of the cluster. In fact Hill's equations state

that there should be no deviation of the cluster from the circular reference orbit. Under the influence of the J_2 disturbance this is not true, and therefore, Hill's equations do a poor job of modeling the cluster's overall motion under the J_2 disturbance.

When modeling the differential motion, Hill's equations fare much better. This is due to the fact that the differential J_2 forces are much smaller when comparing the relative motion of two satellites. However, Hill's equations still failed to capture many of the effects on the satellite motion. The periods of the radial, in-track, and cross-track motion were modeled incorrectly. This resulted in periodic errors of increasing amplitude, and caused the model to break down quickly over time.

Hill's equations also did not incorporate any differential J_2 effects. These effects cause the cluster to drift apart over time and are not captured by Hill's equations.

4.5.1.2 Absolute motion – Solution 1

The 1st solution showed a marked improvement from Hill's equations. Many of the effects that Hill's equations failed to capture were captured with the 1st solution of the new linearized equations: the period of the radial and in-track motion was captured correctly, and the drift in the longitude of the ascending node was also captured.

One problem however was that the cluster and the circular reference orbit drifted away from each other due to a variation in the longitude of the ascending node. While the equations do predict this motion, they eventually break down because of linearization and geometry differences. The solution to this problem was introduced in 2nd solution.

4.5.1.3 Absolute motion – Solution 2

In this solution, the reference orbit was adjusted so that the circular reference orbit and the cluster did not drift apart due to precession of the ascending node. With this change came improvements in model accuracy. The satellite and the reference orbit remained together over time. Some error is introduced in the modeling of the reference orbit. An analytical solution was given for the new circular reference orbit, but this is not a perfect model and errors are present. However, the 2nd solution is an improvement over the 1st

solution. This model predicts the absolute motion with errors on the order of meters to tens of meters per orbit.

4.5.1.4 Absolute motion – Solution 3

In the 3rd solution, the cross-track motion errors were addressed. In these numerical simulations only 'zero' initial conditions were used and there was no cross-track motion. Because of this, the 2nd and 3rd solutions were identical and are not presented.

4.5.1.5 Relative motion

When looking at the shape, size and motion within the cluster, relative motion is used. The new linearized equations are a marked improvement from Hill's equations in terms of modeling the motion of satellites in the cluster. While Hill's equations were not able to predict the period of the radial, in-track, and cross-track direction terms when under the influence of the J_2 disturbance, the new linearized equations of motion were able to successfully capture this motion.

The only significant error arose from a drift in the in-track direction. This was again due to an orbital period mis-match. If the average J_2 disturbance for each satellite could be more accurately determined, this drift could be reduced.

4.5.1.6 Relative motion with correct initial conditions

Every version, including Hill's equations, of the linearized equations of motion suffers from errors. This is due to the fact that the equations are, as the name implies, linearized. They are not exact analytical solutions. Because of this, there is an error in the initial velocity conditions, placing the satellites in the cluster into an orbit with a slightly different orbital period than that of the reference orbit. While the linearized equations of motion do a good job of predicting the zero-drift initial conditions, they are not exact. A drift in the in-track direction develops as a result.

The exact initial conditions for zero drift were calculated and the results are presented. When applied, the linearized equations of motion predicted the correct in-track motion of the satellites without any drift in any of the directions.

Chapter 5

CONCLUSIONS

In this thesis, a need for a new set of linearized equations that capture the J_2 disturbance was identified. These equations were derived in chapter three and verified in chapter four. We will conclude with a discussion on some of the insights that are gained by deriving and using this new set of constant coefficients linearized differential equations of motion.

5.1 The Period of the Relative Orbits

In a satellite cluster, each satellite orbits the center of the cluster in a 'relative orbit'. These relative orbits have a certain period. Hill's equations incorrectly predict that they orbit with the same period as the satellite's orbital period. The new linearized equations of motions state that this is not true under the influence of the J_2 disturbance force. Looking at the in-plane motion ($\hat{x}$ and $\hat{y}$ directions), the period is now

$$P_{rel\ orbit} = \frac{2\pi}{\sqrt{1-s}\ n}$$

where (5.1)

$$s = \frac{3J_2R_e^2}{8r_{ref}^{\ 2}}(1+3\,Cos\,2i_{ref}) \qquad n = \sqrt{\frac{\mu}{r_{ref}^3}}$$

As presented in section 4.1.5, the period of this motion is based upon the length of time between periapsis crossings. Therefore the period of the relative orbit is a combination of the orbital period of the satellite and the rate of precession of the longitude of the ascending node. As discussed in section 4.1.5, the new linearized equations of motion do indeed capture this effect.

5.2 Cross-Track Motion

Cross-Track motion is probably the most complex motion in the cluster. Changes in cross-track motion are due to differential changes in the longitude of the ascending node. As the satellites' orbital planes separate, there is a change in both the period of the $\hat{z}$ terms and the amplitude of the $\hat{z}$ terms. The change in the period of the $\hat{z}$ terms corresponds to the change in location of the intersection of the orbital planes. Changes in the amplitude correspond to the maximum separation of the orbital planes (located 90° away from the intersection of the planes). Clusters that require even spacing of spacecraft around the center of the cluster will have to fight the propensity for the orbital planes to cross at the high latitudes. As the planes separate, the orbital crossing tends to drift away from the equator and approach the poles.

The new linearized equations of motion were adjusted to capture this motion and as shown in chapter 4 do indeed capture this effect of the J_2 disturbance.

5.3 The 'Tumbling' Effect

A satellite's relative orbit is a function of the satellite's relative inclination, eccentricity, longitude of the ascending nose, and argument of periapsis. Under the influence of the J_2 force, these orbital elements undergo changes. Some of these variations cause a change in the orientation of the cluster. This effect has been coined by the author as 'tumbling' because the cluster appears to tumble around the $\hat{z}$ axis. Tumbling is caused by a variation in the argument of periapsis, and differential drift in the longitude of the ascending node.

If we first neglect differential J_2 effects, under the influence of the J_2 disturbance each satellites' argument of periapsis changes at the same rate. As the argument of periapsis changes, the orientation of the cluster also changes, and the cluster tumbles.

If the relative orbit of a satellite follows the locus of points defined by the intersection of a plane with an elliptical cylinder, with the cylinder's axis aligned with the $\hat{z}$ axis, then the tumbling effect causes this plane to rotate about the $\hat{z}$ axis. Figure 5-1 shows the

relative orbit as the intersection of a plane and an elliptical cylinder. This plane is not necessarily perpendicular to the axis of the cylinder. As the argument of periapsis precesses, this plane will rotate about the $\hat{z}$ axis. Therefore the projection in the $\hat{x}-\hat{y}$ plane (Side view) remains undisturbed, while projections in the $\hat{y}-\hat{z}$ and $\hat{x}-\hat{z}$ (Top view and back view respectively) continuously change from an ellipse to a degenerate ellipse (a line) and back again. The rate at which the ellipse tumbles is the same as the rate of change of the argument of periapsis.

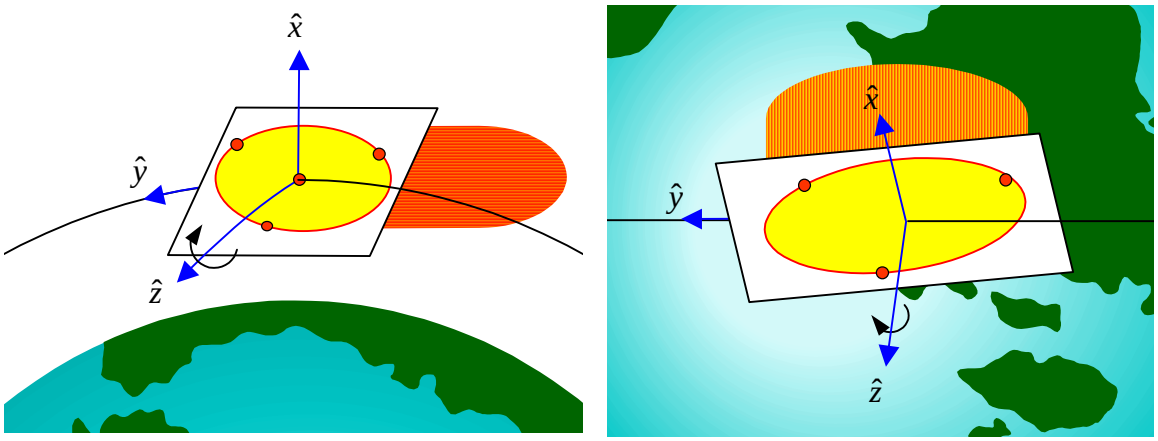

Figure 5-1 : The Relative Orbit

Using the solution to the new linearized equations of motion, tumbling is exhibited by a difference between the period of the $\hat{x}$ and $\hat{y}$ terms and the $\hat{z}$ terms. The period of the $\hat{x}$ and $\hat{y}$ terms is based on the orbital period and the location of the argument of periapsis, while the $\hat{z}$ term is based only on orbital period (ignoring differential effects). This difference in periods is another way of looking at the tumbling effects. As the periodic terms in the $\hat{x}$ and $\hat{z}$ direction become in phase with each other, the projected motion in the $\hat{x}-\hat{z}$ direction becomes a degenerate ellipse. As the two terms move out of phase the ellipse expands until the two terms are 90° out of phase. This process continues as the relative orbits continue to tumble. This motion also happens in the $\hat{y}-\hat{z}$ direction, but when the projection in the $\hat{y}-\hat{z}$ plane is an ellipse, the projection in the $\hat{x}-\hat{z}$ direction is a degenerate ellipse, and vice versa. Motion in the $\hat{x}-\hat{y}$ plane is always

a 2x1 ellipse and does not show any tumbling effects because the $\hat{x}$ and $\hat{y}$ terms have the same period.

Since this tumbling effect is dependent on the period of the $\hat{z}$ terms, changes in the period of the $\hat{z}$ terms will also cause a change in the tumbling rate. If differential J_2 effects are ignored, the $\hat{z}$ terms have the same period as the orbital period (time between equatorial crossings). However, as shown in section 3.6.3 the period of the $\hat{z}$ terms is a function of the differential drift in the longitude of the ascending node, and this must be accounted for when determining the tumbling rate.

For many missions, the correct projection of the cluster towards its target is imperative for mission success. 'Tumbling' will cause this projection to degrade, and either control must be used to counteract this effect or multiple orbit planes must be used so that a 2-D projection is always facing the target.

5.4 Differential Drift in the Cross-Track Direction

In this paper, we have shown that secular drift in each direction, except for differential drift in the longitude of the ascending node, can be eliminated by choosing appropriate initial conditions. This differential drift occurs when satellites are placed into different inclinations. For clusters that contain satellites in different inclinations, active control methods must be applied to keep the cluster together. It can shown, that for a cluster with 500 meter spacing, the worst case Δv needed to keep the cluster together is approximately 5 cm/s/orbit and scales linearly with the size of the cluster.

5.5 Final Comments

In this thesis, a new set of linearized equations of motion that accurately predict relative motion in the presence of the J_2 disturbance force is presented. Past work in the field of formation flying dynamics either uses Hill's equations, or dismisses them as not accurate enough, and a more complex non-linear solution is used. The new linearized equations of

motion will fill this void, and allow cluster designers to easily calculate the motion of spacecraft in a cluster.

These linearized equations of motion were derived in detail in chapter 3. Two interim solutions and a final solution for the absolute motion were presented. These solutions increased in complexity, but at the same time more accurately modeled the effects of the J_2 disturbance force. The relative motion between two satellites or one satellite and the origin of the cluster was also derived and presented. This relative motion turned out to be the homogenous solution to the absolute motion differential equations.

In chapter 4 the new linearized equations of motion were verified in two ways. They were first compared against the mean variation in the orbital elements. The equations were able to capture the mean variation of all six orbital element. Next a numerical simulator was used to verify the equations. Hill's equations were also analyzed and used as a baseline.

The new linearized equations of motion outperformed Hill's equations by orders of magnitude. The errors incurred by the new linearized equations of motion were on the order of centimeters. The only significant error was the drift in the in-track direction. The new linearized equations of motion were not able to exactly predict the correct initial velocity. This is due to the fact that they are not exact equations of motion but instead linearized equations of motion.

Because of this error, and the sensitivity to initial velocity conditions, there was a drift in the in-track direction of a few meters per orbit. To fix this problem, a method of calculating the correct initial velocity was presented for satellites in the same orbital plane. For other satellites, a numerical method was used. This initial condition problem is one area that is left open for future work. However, once the correct initial conditions are used, the error in the in-track direction should be on the order of centimeters.

Finally, in this thesis we have successfully presented a new set of linearized, constant coefficient differential equations that are as simple in form as Hill's equations, but also capture the effect of the J_2 disturbance force. It is hoped that these equations will become a valuable tool for satellite formation flying.

REFERENCES

[1] R.J. Sedwick, D.W. Miller, E.M.C. Kong, “Mitigation of Differential Perturbations in Clusters of Formation Flying Satellites,” AAS 99-124.

[2] http://info.aoc.nrao.edu/vla/html/vlahome/vlaoverview.html

[3] John E. Prussing, Bruce A. Conway, *Orbital Mechanics*, Oxford University Press, New York, 1993.

[4] Mark V. Tollefson, “Relative Orbit Design Tool,” Presented at the IEEE Aerospace Conference, 2001.

[5] E. Kong, M. Tollefson, J. Skinner, J. Rosenstock, “TechSat 21 Cluster Design Using AI Approaches and the Cornwell Metric,” AIAA 99-4365.

[6] H. Yeh, A. Sparks, “Geometry and Control of Satellite Formations”, Proceedings of the American Control Conference, Chicago, IL, June 2000.

[7] Chris Sabol, Richard Burns, Craig A. McLaughlin, “Satellite Formation Flying Design and Evolution,” AAS 99-121.

[8] A. Sparks, “Linear Control of Satellite Formation Flying”, AIAA-2000-4438

[9] K. Alfriend, H. Schaub, D. Gim, “Gravitational Pertubations, Nonlinearity and Circular Orbit Assumption Effects on Formation Flying Control Strategies,” AAS 00-12.

[10] D. Lawdin, “Optimal Trajectories for Space Navigation,” Butterworths, London, 1963.

[11] G. Inalhan, J. How, “Relative Dynamics & Control of Spacecraft Formations in Eccentric Orbits,” AIAA-2000-4443.

[12] H. Schaub, K. Alfriend, “J_2 Invariant Relative Orbits for Spacecraft Formations,” NASA GSFC Flight Mechanics and Estimation Conference, May 1999.

[13] H. Schaub, K. Alfriend, “Impulsive Spacecraft Formation Flying Control to Establish Specific Mean Orbital Elements,” AAS 00-113

[14] R. Sedwick, D. Miller, E. Kong, “Mitigation of Differential Perturbations in Clusters of Formations Flying Satellites”, AAS 99-124.

[15] S. A. Schweighart, R. J. Sedwick, “A Perturbative Analysis of Geopotential Disturbances for Satellite Formation Flying,” Presented at the IEEE Aerospace Conference, 2001.

[16] Edmund M. C. Kong, David W. Miller, Raymond J. Sedwick, “Exploiting Orbital Dynamics for aperture Synthesis Using Distributor Satellite Systems: Applications to a Visible Earth Imager System,” AAS 99-122.

[17] D. Stansbery, J. Cloutier, “Nonlinear Control of Satellite Formation Flight,” AIAA Guidance, Navigation, and Control Conference and Exhibit, August 2000, AIAA-2000-4436.

[18] R. Battin, *An Introduction to the Mathematics and Methods of Astrodynamics*, American Institute of Aeronautics and Astronautics, Inc., New York, 1987.